

1 ~~The underappreciated impact of emission source profiles on the simulation of~~
2 ~~PM_{2.5} components: New evidence from sensitivity analysis~~The effect of emission
3 source chemical profiles on simulated PM_{2.5} components: sensitivity analysis
4 with CMAQv-5.0.2

5 Zhongwei Luo^{a,b,1}, Yan Han^{a,b,c,1}, Kun Hua^{a,b}, Yufen Zhang^{a,b*}, Jianhui Wu^{a,b}, Xiaohui
6 Bi^{a,b}, Qili Dai^{a,b}, Baoshuang Liu^{a,b}, Yang Chen^c, Xin Long^c, Yinchang Feng^{a,b*}

7 ^aState Environmental Protection Key Laboratory of Urban Ambient Air Particulate
8 Matter Pollution Prevention and Control & Tianjin Key Laboratory of Urban
9 Transport Emission Research, College of Environmental Science and Engineering,
10 Nankai University, Tianjin 300350, China.

11 ^bCMA-NKU Cooperative Laboratory for Atmospheric Environment-Health Research,
12 Tianjin 300350, China.

13 ^cResearch Center for Atmospheric Environment, Chongqing Institute of Green and
14 Intelligent Technology, Chinese Academy of Sciences, Chongqing 400714, China.

15
16
17 *Corresponding authors:

18 Y. F. Zhang (zhafox@nankai.edu.cn). And Y. C. Feng (fengyc@nankai.edu.cn).

19
20 ¹Z. W. Luo and Y. Han equally contribute to this work

21 **Abstract**

22 The chemical transport model (CTM) is an essential tool for air quality prediction
23 and management, widely used in air pollution control and health risk assessment.
24 However, the current models do not perform very well in reproducing the observations
25 of some major chemical components, for example, sulfate, nitrate, ammonium and
26 organic carbonsimulating PM_{2.5} components. Studies suggested that the uncertainties
27 of model chemical mechanism, source emission inventory and meteorological field can
28 cause inaccurate simulation results. Still, the emission source profile (used to create
29 speciated emission inventories for CTMs) of PM_{2.5} has not been fully taken into account
30 in current numerical simulation. This study aims to answer (1) Whether the variation of
31 source profile adopted in CTMs has an impact on the simulation of PM_{2.5} chemical
32 components? (2) How much does it impact? (3) How does the impact work? Based on
33 the characteristics and variation rules of chemical components in typical PM_{2.5} sources,
34 different simulation scenarios were designed and the sensitivity of simulated PM_{2.5}
35 componentselements simulation results to PM_{2.5} sources chemical profile was
36 explored. Our findings showed that the influence of source profile changes on simulated
37 PM_{2.5} concentration was insignificant, but its impact on simulated PM_{2.5} components
38 could not be ignored. The variations of simulated components ranged from 8% to 167%
39 under selected different source profiles, and simulation Simulation results of some
40 components were sensitive to the adopted PM_{2.5}-source profile in CTMs. Moreover,
41 there was a linkage effect, the variation of some components in the source profile would
42 bring changes to the simulated results of other components. These influences are
43 connected to ~~the~~ chemical mechanisms of the model since the variation of species
44 allocations in emission sources directly affected the can affect potential composition
45 and phase state of aerosols, chemical reaction priority and multicomponent chemical
46 balance in thermodynamic equilibrium system. We also found that the perturbation of
47 the PM_{2.5} source profile caused the variation of simulated gaseous pollutants, which
48 indirectly indicated that the perturbation of ~~the~~ source profile would affected the

49 simulation of secondary PM_{2.5} components. Given the vital role of air quality simulation
50 in environment management and health risk assessment, the representativeness and
51 timeliness of source profile should be considered.

52 **Keywords**

53 PM_{2.5}; source profile; component; numerical simulation; chemical transport model

54 **1. Introduction**

55 Ambient fine particulate matter (PM_{2.5}) pollution in some key regions of China
56 has attracted much attention (Liang et al., 2020; Huang et al., 2021). The chemical
57 components of PM_{2.5}, including elements (Al, Si, Fe, Mn, Ti, Cu, Zn, Pb, etc.), water-
58 soluble ions (SO₄²⁻, NO₃⁻, Cl⁻, F⁻, NH₄⁺, Na⁺, K⁺, Mg²⁺, Ca²⁺, etc.), and carbon-
59 containing components (Organic Carbon, OC; Elemental Carbon, EC) (Yang et al.,
60 2011; Li et al., 2013), have different physical and chemical properties, such as reactivity,
61 thermal stability, particle size distribution, residence time, optical properties, health
62 hazards, etc (Seinfeld and Pandis, 2006; Tang et al., 2006). According to long-term
63 monitoring results, in most regions of China, SO₄²⁻, NO₃⁻, NH₄⁺ and OC are the most
64 important species in ambient PM_{2.5} (Li et al., 2017a; Li et al., 2021), which has a certain
65 adverse impact on human health (Shi et al., 2018) and ecosystem, such as acid rain in
66 southwest China (Han et al., 2019), food security (Zhou et al., 2018), etc.

67 The chemical transport models (CTMs) play an important role in policy making
68 for regulatory purposes. Based on the scientific understanding of atmospheric physical
69 and chemical processes, CTMs are built to simulate the transport, reaction and removal
70 of pollutants on a certain scale in horizontal and vertical directions. With the
71 development of CTMs, the simulation accuracy of PM_{2.5} concentration has been
72 significantly improved. Higher requirements have been put forward for the precise
73 simulation of PM_{2.5} components so as to provide support for the use of CTMs in human
74 health risk assessment, climate effects, pollution sources apportionment, and so on
75 (Peterson et al., 2020; Lv et al., 2021). However, the current models perform not very
76 well in simulating some components (for example, PM_{2.5}-bound sulfate, nitrate,
77 ammonium, trace elements, etc.) (Zheng et al., 2015; Fu et al., 2016; Ying et al., 2018;
78 Cao et al., 2021). In the current literatures, the correlation coefficient (R) and
79 normalized mean bias (NMB) are highly variable and inconsistent between the
80 simulated and the observed values (listed in Table S1). This is mainly attributable to the
81 uncertainties of model chemical mechanism, source emission inventory and

82 meteorological field simulation.

83 The chemical mechanisms involved in CTMs are derived from parameterized
84 assumptions based on laboratory simulation and field observations. The actual
85 atmospheric chemical processes are very complex, and some reaction mechanisms are
86 still limitedly understood. In addition, the integration of chemical reactions and
87 simplified treatment methods in the model cannot fully reflect the correlation among
88 atmospheric pollutants. For example, in some model mechanisms, ~~other~~-important
89 sulfate and nitrate formation pathways through new heterogeneous chemistry were
90 added ~~through new heterogeneous chemistry~~, including the chemical reaction between
91 SO₂ and aerosol, NO₂/NO₃/N₂O₃ and aerosol (Zheng et al., 2015), nitrous acid oxidized
92 SO₂ to produce sulfate (Zheng et al., 2020), dust particles promoted the oxidation of
93 SO₂ (Yu et al., 2020), modified the uptake coefficients for heterogeneous oxidation of
94 SO₂ to sulfate (Zhang et al., 2019), updated the heterogeneous N₂O₅ parameterization
95 (Foley et al., 2010). Even though the aforementioned processes can significantly
96 improve the simulation of SO₄²⁻ and NO₃⁻, there is still a gap between the modeled and
97 the actual atmospheric chemical processes.

98 ~~The uncertainty of source emission inventory also significantly affects the~~
99 ~~simulation results of PM_{2.5} components (Shi et al., 2017; Sha et al., 2019). Due to~~
100 ~~incomplete information or insufficient representativeness, pollutant emissions are~~
101 ~~sometimes overestimated or underestimated, and the method for temporal and spatial~~
102 ~~allocation also needs to be improved.~~

103 The uncertainty of meteorological field simulation is another crucial reason for the
104 simulation deviation, especially on heavy pollution days, the variation trends of PM_{2.5}
105 chemical components were not well-captured (Ying et al., 2018; Qi et al., 2019; Wang
106 et al., 2022). Precipitation is the key meteorological factor determining wet removal of
107 pollutants; boundary layer height and wind speed are the main factors affecting
108 convection and transport of pollutants; solar radiation, temperature and relative
109 humidity are the key factors affecting the formation of secondary particles (Huang et
110 al., 2019; Chen et al., 2020). Some literature reported that deviation from precipitation

111 and wind field simulation might lead to underestimation of SO_4^{2-} , NO_3^- and NH_4^+
112 (Cheng et al., 2015; Zhang et al., 2017). Devaluation of liquid water path and cloud
113 cover cause a decrease of sulfate formation in cloud, and ultimately results in
114 significantly underestimated components in simulation values (Sha et al., 2019; Foley
115 et al., 2010). Underestimation of temperature and relative humidity may also cause
116 adverse effects of temperature- and/or relative humidity-dependence chemical reaction
117 in the simulation (Sha et al., 2019).

118 The uncertainty of source emission inventory also significantly affects the
119 simulation results of $\text{PM}_{2.5}$ components (Shi et al., 2017; Sha et al., 2019). Due to
120 incomplete information or insufficient representativeness, pollutant emissions are
121 sometimes overestimated or underestimated, and the method for temporal and spatial
122 allocation also needs to be improved.

123 In particular, the emission source profile of $\text{PM}_{2.5}$ (Hereinafter referred to as
124 "source profile"), used to creating speciated emission inventories for CTMs (Hsu et
125 al., 2019), has not been fully taken into account in the current numerical simulation. In
126 the reported literatures, $\text{PM}_{2.5}$ species allocation coefficients of emission sources are
127 commonly treated in the following ways: (1) allocated $\text{PM}_{2.5}$ components of source
128 emissions by referring to source profile data in published literature or database like the
129 US SPECIATE (Fu et al., 2013; Wang et al., 2014; Ying et al., 2018); (2) chemical
130 profiles come from local measurement (Fu et al., 2013; Appel et al., 2013). However,
131 with the development of production technology and the innovation of pollution
132 treatment technology in recent years, some source profiles have changed dramatically
133 (Bi et al., 2019), such as SO_4^{2-} from coal burning, SO_4^{2-} content in $\text{PM}_{2.5}$ is generally
134 low in coal-fired power plant without desulfurizing facilities, while existing coal-fired
135 power plants using limestone/gypsum wet desulphurization, the contents of SO_4^{2-} in
136 $\text{PM}_{2.5}$ are significantly higher than that without desulfurization facilities (Zhang et al.,
137 2020). The timeliness of $\text{PM}_{2.5}$ species allocation coefficients in current CTMs also
138 needs to be considered.

139 This paper attempts to answer the following questions: (1) Whether the variation

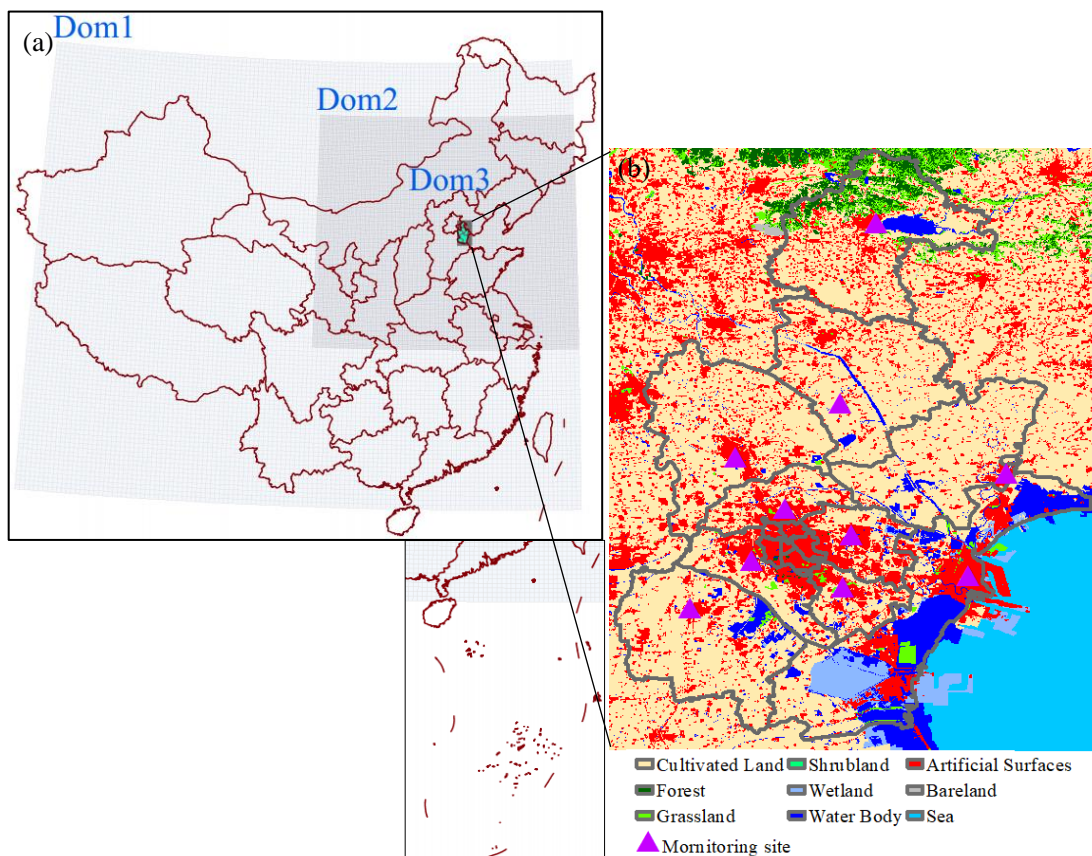
140 of the source profile adopted in the ~~air quality~~ model has an impact on the simulated
141 results of PM_{2.5} chemical components? (2) How much does it impact? (3) How does
142 the impact work? Aiming at these problems above, chemical composition and its
143 variation law for typical PM_{2.5} emission sources are summarized, on this basis,
144 sensitivity tests are designed to identify whether PM_{2.5} source profiles and species
145 allocation in the model are important parameters that affect the simulation results of
146 chemical components in PM_{2.5}. We take CMAQ (one of the most widely used CTMs),
147 MEIC (a high-resolution inventory of anthropogenic air pollutants in China) as the
148 carriers. The same kind of experiment is also applicable to other CTMs and emission
149 inventories. The aim of this study is to provide support for the effective utilization of
150 source profiles in the CTMs and improvement of the simulation schemes.

151 2. Model and Data

152 2.1 Model configuration

153 Weather Research and Forecasting model (WRF-3.7.1), the widely used
154 Community Multiscale Air Quality model (CMAQv5.0.2), and Multi-resolution
155 Emission Inventory for China (MEICv1.3) have been used in this study. MEIC_
156 ~~developed by Tsinghua University provided the emission inventory which is developed~~
157 ~~by Tsinghua University~~, mainly tracked anthropogenic emissions in China including
158 coal-fired power plants, industry, vehicles, residents and agriculture
159 (http://meicmodel.org/?page_id=135) (Li et al., 2017b; Zheng et al., 2018). The WRF
160 model was used to generate meteorological inputs for the CMAQ model. Three nested
161 modeling domains consisting of 36 km×36 km (Dom1), 12 km×12km (Dom2), and 4
162 km×4km (Dom3) horizontal grid sizes were set, as shown in Fig. 1. The initial and
163 boundary conditions for WRF were based on the North American Regional Reanalysis
164 data archived at National Center for Atmospheric Research (NCAR). In addition,
165 surface and upper air observations obtained from NCAR were used to further refine the
166 analysis data. ~~The modeling was conducted from Oct. 1 to Oct.30 in 2018, The and~~
167 major configurations we used in CMAQ were illuminated as follows: Gas-phase

168 chemistry was based on the CB05 mechanism and the aerosol dynamics/chemistry was
169 based on the aero6 module (cb05tucl_ae6_aq). The detailed model configurations were
170 shown in Table S2, and regional distribution of PM_{2.5} emission sources were shown in
171 Fig-ure S2S1.



172
173 Fig.1 Modeling domains of the CMAQ model. (a) The three-domain nested CMAQ domains; (b)
174 Land use and observation sites of Dom3 (Data source of Land use: GLOBELAND30,
175 www.globeland30.org, National Geomatics Center of China).

176 2.2 Selection and comparison of PM_{2.5} emission source profile

177 The PM_{2.5} emission source profiles from database of Source Profiles of Air
178 Pollution (SPAP) (<http://www.nkspap.com:9091/>), U.S. Environmental Protection
179 Agency's (EPA) SPECIATE database (<https://www.epa.gov/air-emissions-modeling/speciate>) as well as from published literature were selected, respectively. The
180 SPAP was developed by the State Environment Protection Key Laboratory of Urban
181 Particulate Air Pollution Prevention, Nankai University, China. This database contains
182 more than 3000 size-resolved source profiles of stationary combustion sources,
183 industrial processes, vehicle exhaust, biomass burning, dust and ~~cooking emissions and~~

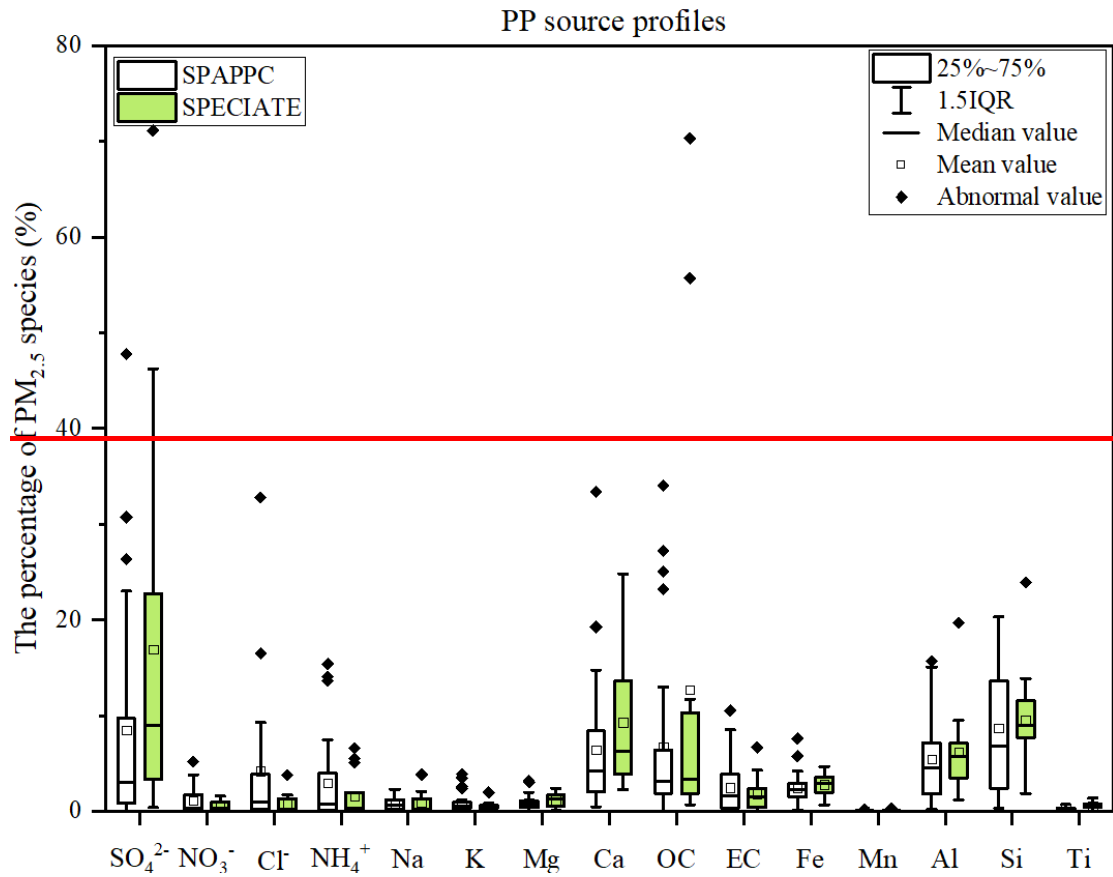
185 other sources, collected from more than 40 cities in China since 2001. In addition to
 186 inorganic elements, water-soluble ions, OC, EC and other conventional components,
 187 some source profiles also encompass a series of tracer information, such as organic
 188 markers, isotopes, single particle mass spectrometry, VOCs and other gaseous
 189 precursors. Based on species in the aerosol chemical mechanism (AERO6) of CMAQ
 190 (Appel et al., 2013; Chapel Hill, 2012), we selected 15 components in PM_{2.5} source
 191 profiles including Al, Ca, Cl, EC, Fe, K, Mg, Mn, Na, OC, Si, Ti, NH₄⁺, NO₃⁻ and SO₄²⁻,
 192 the remaining components are classified as “other”. ~~Emission sources are divided into~~
 193 ~~four main categories referred to the classification in MEIC: coal combustion by power~~
 194 ~~plants (PP), industrial processes (IN), residential emission (RE) and transportation~~
 195 ~~sector (TR). In the database of Source Profiles of Air Pollution (SPAP) and U.S.~~
 196 ~~Environmental Protection Agency’s (EPA) SPECIATE database, these four source~~
 197 ~~categories (coal-fired power plant, industry process, transportation sector and~~
 198 ~~residential coal combustion) contain a series of sub-categories. But the MEIC emission~~
 199 ~~inventory does not include the corresponding sub-categories. So we take the average~~
 200 ~~values of source profiles in each source category as representing source profile, the~~
 201 ~~details could also be seen in our previous work (Bi et al., 2019); Then multiply~~
 202 ~~inventory emissions by profile fraction to get emissions of specific chemical~~
 203 ~~components.~~

204 To determine the similarity between the two groups of source profiles, Coefficient
 205 Divergence (CD) is calculated using the following formula (Wongphatarakul et al.,
 206 1998):

$$CD_{jk} = \sqrt{\frac{1}{p} \sum_{i=1}^p \left(\frac{x_{ij} - x_{ik}}{x_{ij} + x_{ik}} \right)^2} \dots\dots\dots (1)$$

208 Where CD_{jk} is the coefficient of divergence of source profile j and k, p was is the
 209 number of chemical components in source profile, x_{ij} is the weight percentage for
 210 chemical component i in source profile j, x_{ik} is the weight percentage for i in source
 211 profile k (%). The CD value is in the range of 0 to 1, if the two source profiles are
 212 similar, the value of CD is close to 0; if the two are very different, the value was is close

213 to 1.
214 Coal-fired power plant (PP). Coal-fired power plants—remain the main coal
215 consumers in China, which accounted for 50.2% of total coal consumption in 2019
216 (NBS, 2021) and gained much more attention, especially with the wide implementation
217 of the ~~strictest~~—ultralow emission standards, PM_{2.5} emission characteristics have
218 changed accordingly (Wu et al., 2020; Wu et al., 2022). There are obvious differences
219 in PM_{2.5} source profiles between SPAPPC (SPAP database and published source profiles
220 in China) and SPECIATE (U.S.EPA SPECIATE database), the CD value of these two
221 groups lie between 0.34 and 0.92 (0.64±0.10), detailed information is shown in Table
222 S3 and Figure S2. The percentages of species in PP source profiles are plotted in Fig.
223 2(a). The main components in SPAPPC are sorted by Si, SO₄²⁻, OC, Ca with average
224 values of 8.7±6.8%, 8.5±11.5%, 6.8±9.1% and 6.5±6.9%, respectively; The SPECIATE
225 are enriched in SO₄²⁻ (16.9%±20.0%), OC (12.7±21.8%), Si (9.6±5.0%) and Ca
226 (9.3±7.3%), higher than SPAPPC. Coal properties, burning conditions, pollution control
227 measures and emission sampling methods are the main reasons for those great
228 percentage fluctuations. Different treatment processes of flue gases, e.g. wet/dry
229 limestone, ammonia and double-alkali flue gas desulfurization, will affect the
230 percentages of components in source profiles (Zhang et al., 2020). It has been reported
231 that the percentage of Ca, Mg, SO₄²⁻ and Cl⁻ in PP profiles increased after the limestone-
232 gypsum method was used in coal-fired power plants (Bi et al., 2019). Besides that, the
233 percentage of Cl⁻ in SPAPPC is obviously higher than that in SPECIATE, which might
234 attribute to the generally higher Cl⁻ content in raw coal in China (Guo et al., 2004).



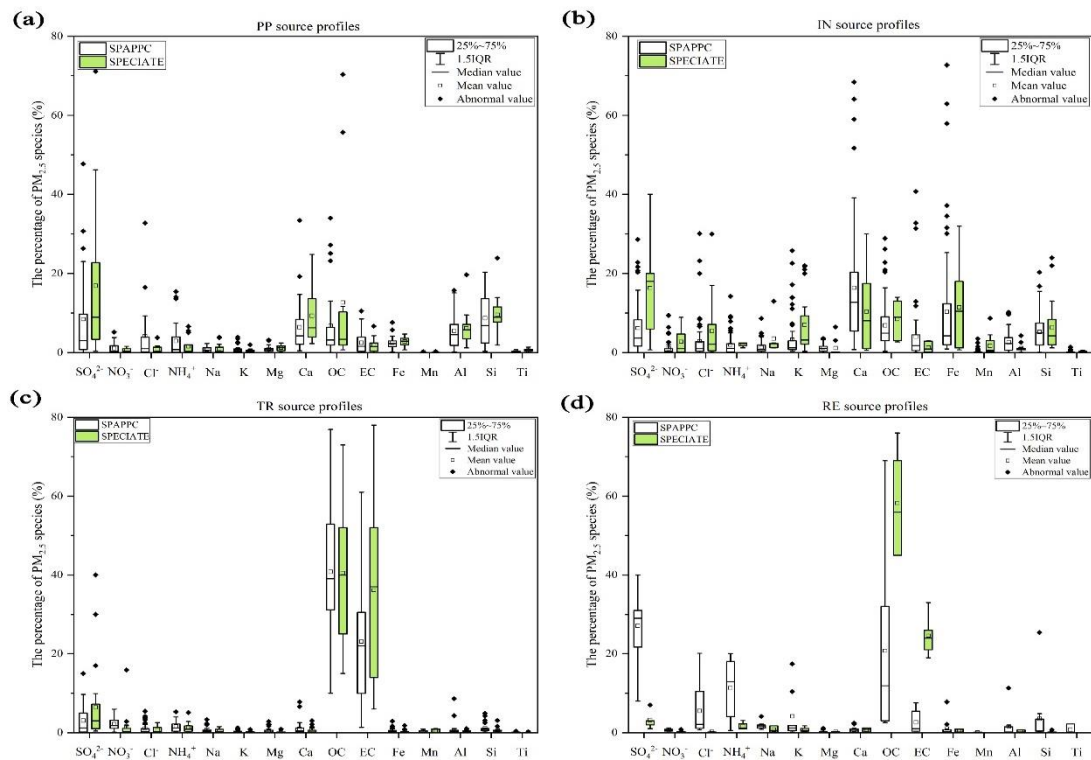
235

236

237

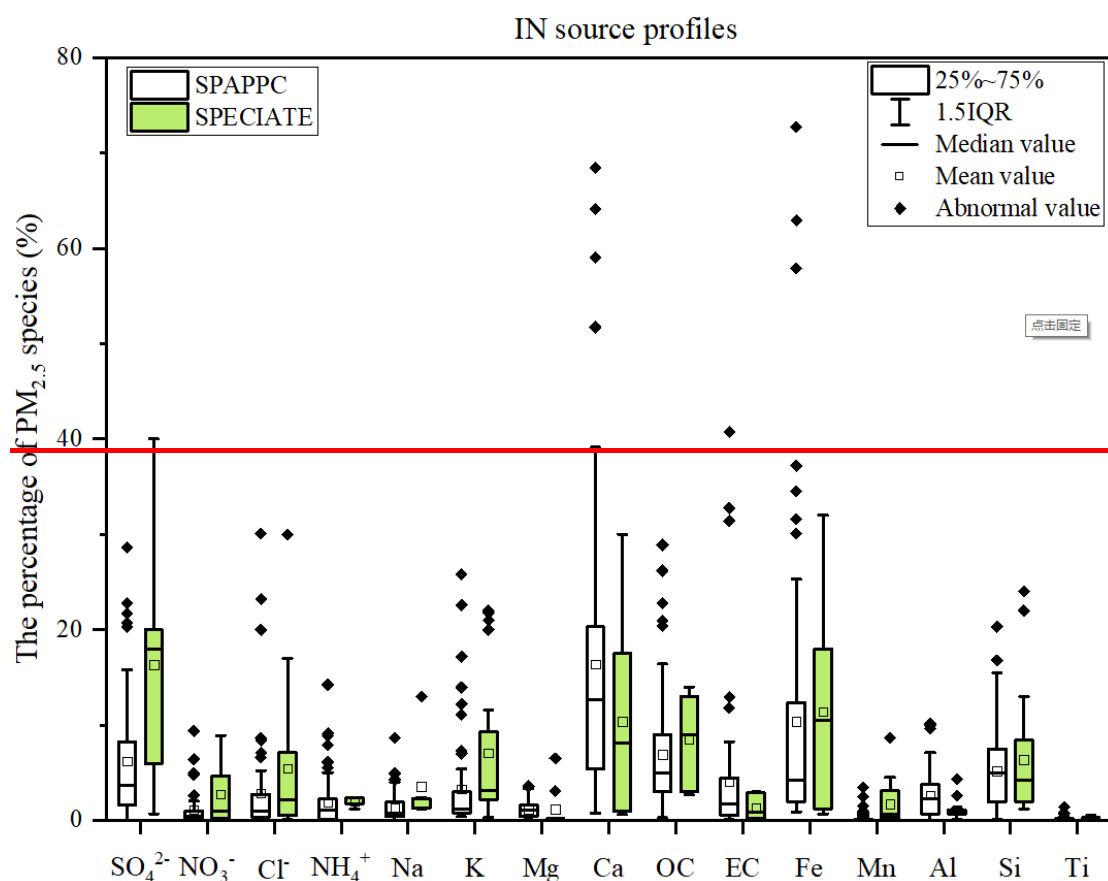
238

Fig. 2 Chemical profiles for PM_{2.5} emitted from coal-fired power plant (PP). Data obtained from SPAPPC (SPAP database and published source profiles in China) and SPECIATE (U.S. EPA SPECIATE database)



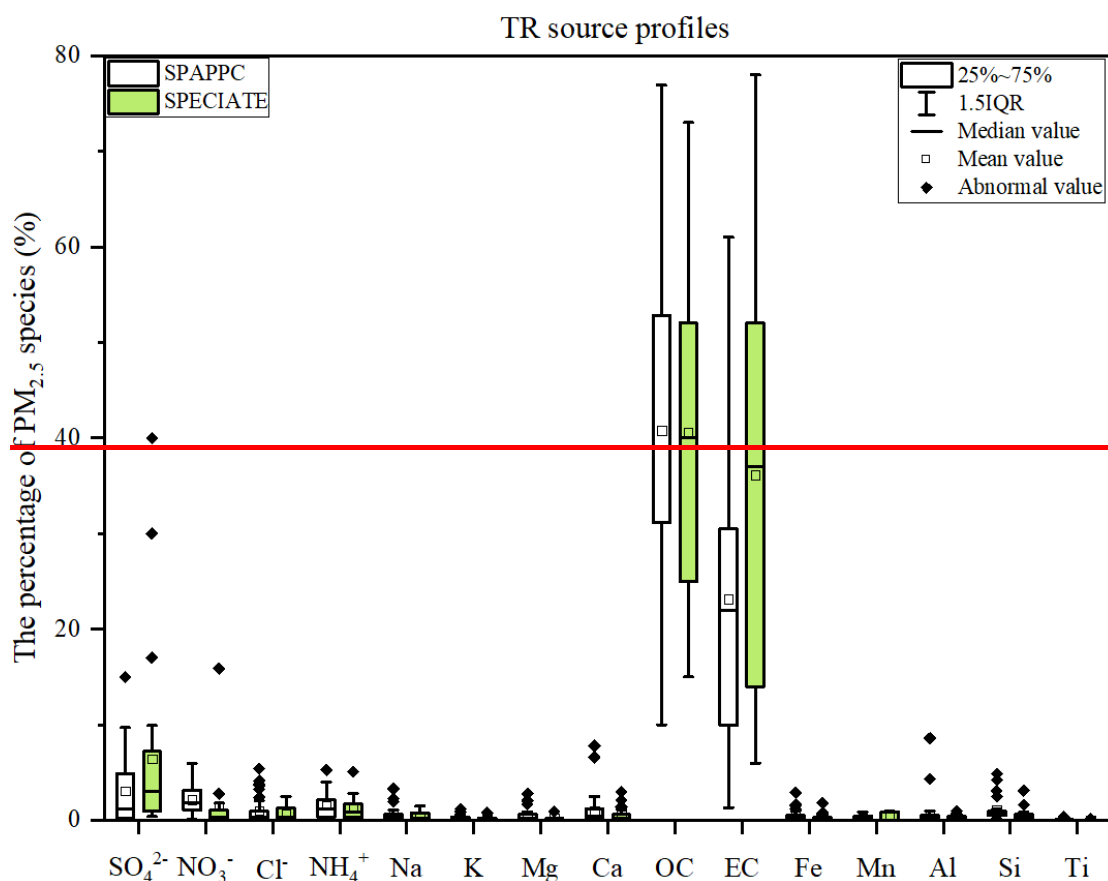
239
240 **Fig. 2** Chemical profiles for PM_{2.5} emitted from (a) coal-fired power plants (PP), (b) industry
241 processes (IN), (c) transportation sector (TR), (d) residential coal combustion (RE). Data obtained
242 from SPAPPC (SPAP database and published source profiles in China) and SPECIATE (U.S. EPA
243 SPECIATE database)

244 **Industrial process(IN).** Industrial emissions are one of the major sources of PM_{2.5}
245 (Hopke et al., 2020), the percentages of Ca, Fe, OC and SO₄²⁻ are relatively high both
246 in SPAPPC and SPECIATE ~~of industrial processes~~, but the shares in different source
247 profile database varied, their CD values vary from 0.45 to 0.94 (0.72±0.09) (Detailed
248 information were shown in Table S4~S7 and Figure S3). In SPAPPC, these four
249 components account for 16.4±14.9%, 10.4±14.4%, 6.9±6.1%, 6.2±6.4%, the
250 proportions in SPECIATE are 10.4±9.8%, 11.4±10.6%, 8.5±4.9%, 16.3±13.3%,
251 respectively (Fig. [32\(b\)](#)). Large variations of components and their percentages in
252 industrial processes are attributed to the manufacturing processes, raw material,
253 pollution control measures and so on (Ji et al., 2017; Bi et al., 2019; Gao et al., 2022).
254 For example, Ca, Al, OC and SO₄²⁻ are found to have the highest percentage in cement
255 sources (Guo et al., 2021); Fe, Si and SO₄²⁻ are the most abundant species in steel
256 industry emission (Guo et al., 2017).



257
258 ~~Fig. 3 Chemical profiles for PM_{2.5} emitted from industry processes (IN). Data obtained from~~
259 ~~SPAPPC (SPAP database and published source profiles in China) and SPECIATE (U.S. EPA~~
260 ~~SPECIATE database)~~

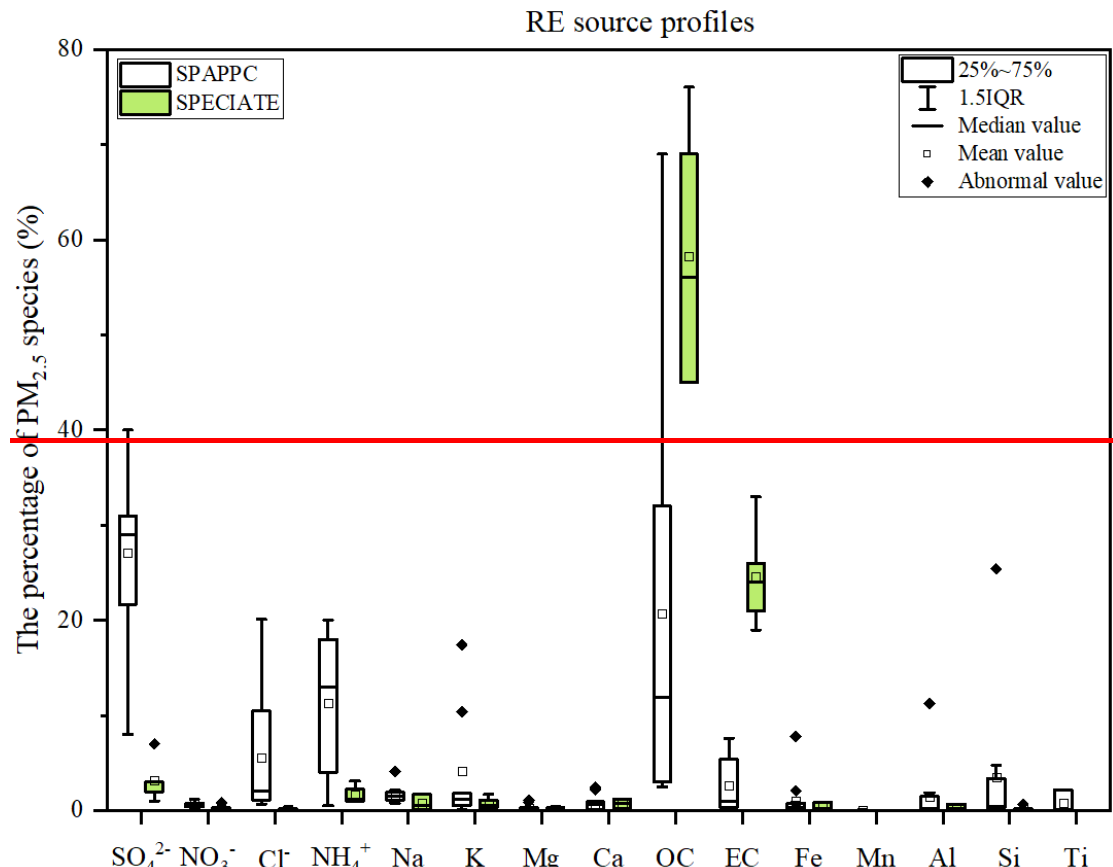
261 **Transportation sector (TR).** Traffic contributed a large fraction of PM_{2.5} in many
262 locations (Hopke et al., 2022). It is well-known that the transportation sector makes a
263 dominant contribution of OC and EC. The main components of PM_{2.5} emitted from
264 traffic sources are OC, EC and SO₄²⁻ both in SPAPPC and SPECIATE, but still vary in
265 wide range, their CD values fall between 0.33 and 0.86 (0.69±0.09) (Detailed
266 information was given in Table S8~S10 and Figure S4). In SPAPPC, the percentages of
267 OC, EC and SO₄²⁻ are 40.8±15.0%, 23.1±13.8%, 3.1±3.7%, and in SPECIATE, the
268 percentages are 40.6±16.4%, 36.1±21.5%, 6.4±9.9%, respectively (Fig. 42(c)). These
269 significant differences mainly attribute to the vehicle type, fuel quality, mixing ratio
270 between oil and gas and the combustion phase in vehicle engine and so on (Xia et al.,
271 2017).



272 Fig. 4 Chemical profiles for PM_{2.5} emitted from transportation sector (TR). Data obtained from
 273 SPAPPC (SPAP database and published source profiles in China) and SPECIATE (U.S. EPA
 274 SPECIATE database)
 275

276 **Residential coal combustion (RE).** Residential coal combustion, as the leading
 277 source of global PM_{2.5} emission (Weagle et al., 2018), has a much higher emission
 278 factor than coal-fired power plant (Wu et al., 2022). The fraction of components **varied**
 279 **vary** greatly in the profiles measured from SPAPPC and SPECIATE, **their CD values**
 280 **are 0.75±0.10** (Detailed information was given in Table S11 **and Figure S5**), SO₄²⁻, OC,
 281 NH₄⁺ and EC make the main contribution to PM_{2.5} emitted from residential coal
 282 combustion. In SPAPPC, the average percentages of SO₄²⁻, OC, NH₄⁺, EC are
 283 27.1±10.1%, 20.7±20.6%, 11.3±7.7%, 2.6±2.8%, respectively. In SPECIATE, the
 284 average percentages are OC (58.2±14.0%), EC (24.6±5.4%), SO₄²⁻ (3.2±2.3%) and
 285 NH₄⁺ (1.6±1.0%) (Fig. **S2(d)**). Total percentages of OC and EC in SPECIATE are over
 286 80%, obviously higher than that in SPAPPC, while a higher percentage of SO₄²⁻, Cl⁻, K,
 287 and Si are observed in SPAPPC. The coal type and properties, burning condition are the
 288 main factors affecting the percentages of PM_{2.5} components, like the chunk coal burning

289 has relatively higher percentages of OC, EC, SO_4^{2-} , NO_3^- and NH_4^+ than honeycomb
 290 briquette (Wu et al., 2021; Song et al., 2021).



291
 292 **Fig. 5 Chemical profiles for $\text{PM}_{2.5}$ emitted from residential coal combustion (RE). Data obtained**
 293 **from SPAPPC (SPAP database and published source profiles in China) and SPECIATE (U.S. EPA**
 294 **SPECIATE database)**

295 Briefly, many factors can affect $\text{PM}_{2.5}$ source profiles, and with the innovation of
 296 manufacturing technique and pollution control technology, changes in fuel and raw and
 297 auxiliary materials, the main chemical components and their percentages would change
 298 dramatically. To explore whether the variations of source profile adopted in CMAQ
 299 model would be one of the important factors affecting the simulation-simulated results
 300 of $\text{PM}_{2.5}$ species-component in CTMs, we designed a series of simulation tests to address
 301 the following issues as follows.

302 **3 ~~Whether the variation of source profile adopted in CTMs has an impact on the~~**
303 **~~simulation of chemical components in PM_{2.5}? Is there an impact of variation of~~**
304 **~~source profile on the simulation results?~~**

305 In this part, we separately selected source profiles from SPAPPC and SPECIATE
306 databases and applied them in emission inventory for simulating PM_{2.5} and its
307 components with other modeling conditions unchanged, corresponding to case
308 CMAQ_SPA and CMAQ_SPE. The detailed information of source profiles is shown in
309 Figure S1S6. ~~To determine the similarity between the two groups of source profiles,~~
310 ~~Coefficient Divergence (CD) is calculated using the following formula~~
311 ~~(Wongphatarakul et al., 1998):~~

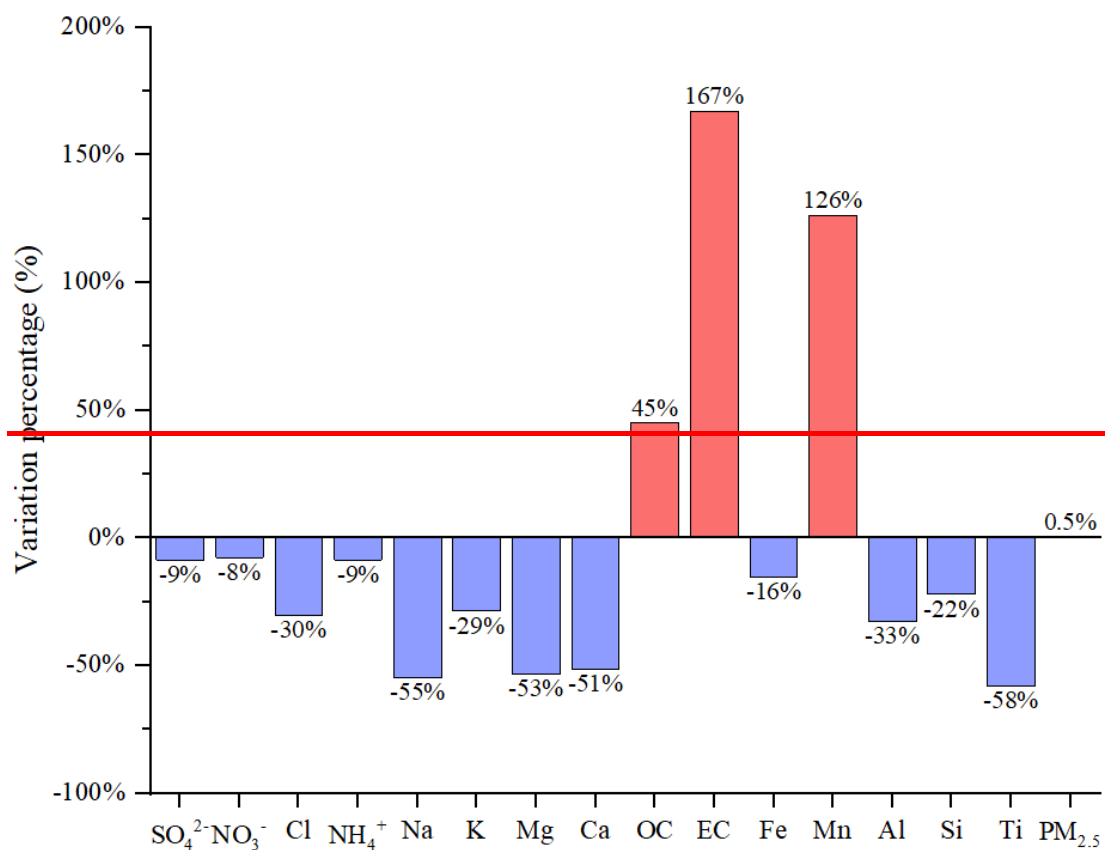
$$312 \quad CD_{jk} = \sqrt{\frac{1}{p} \sum_{i=1}^p \left(\frac{x_{ij} - x_{ik}}{x_{ij} + x_{ik}} \right)^2} \dots\dots\dots (1)$$

313 ~~Where CD_{jk} is the coefficient of divergence of source profile j and k, p was the~~
314 ~~number of chemical components in source profile, x_{ij} is the weight percentage for~~
315 ~~chemical component i in source profile j, x_{ik} is the weight percentage for i in source~~
316 ~~profile k (%). The CD value is in the range of 0 to 1, if the two source profiles are~~
317 ~~similar, the value of CD is close to 0; if the two are very different, the value was close~~
318 ~~to 1.~~

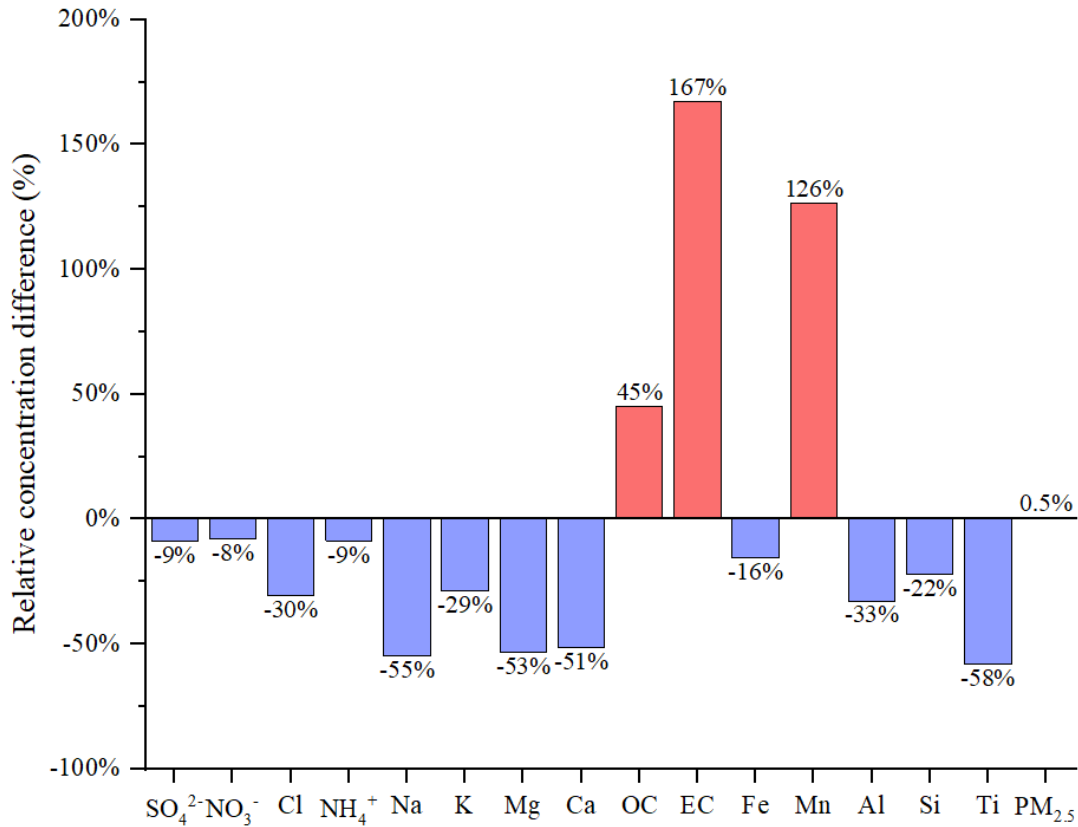
319 By comparing the selected SPAPPC source profiles with the selected SPECIATE
320 source profiles, the coefficient divergences for the four main source categories were
321 CD_{PP}(0.67)>CD_{RE}(0.62)>CD_{TR}(0.60)>CD_{IN}(0.60), which meant the selected source
322 profiles in the two simulation cases were quite different. The average simulated
323 concentration of PM_{2.5} and its components at each 10 ambient air quality monitoring
324 stations (Table S12) were extracted from CMAQ outputs, ~~of the innermost simulation~~
325 ~~domain.~~ We selected one air quality monitoring station (Site 8, as the selected station
326 here and any one site could be available) to explore the effect of emission source
327 chemical profiles on simulated PM_{2.5} components~~study the influence of PM_{2.5} source~~
328 ~~profile on numerical simulation of PM_{2.5}-bound components and to explore the relevant~~
329 ~~laws in the atmosphere~~, then used the left 9 sites to further illustrate the conclusions

330 suggested.

331 The simulation results for PM_{2.5} species under CMAQ_SPA and CMAQ_SPE
332 cases also showed big differences (as shown in Fig. 6-3 and Table S13), in which the
333 The largest difference in average simulated concentration was EC with CAMQ_SPE
334 giving higher by 167% than CMAQ_SPA; For OC and Mn, higher values were also
335 given by CMAQ_SPE than by CMAQ_SPA (45% and 126% on average, respectively);
336 For the remaining other components of concern, the simulated concentration by
337 CMAQ_SPE was lower than CMAQ_SPA with Ti (58%), Na (55%), Mg (53%), Ca
338 (51%), Al (33%), Cl (30%), K (29%), Si (22%), Fe (16%), NH₄⁺ (9%), SO₄²⁻ (9%), NO₃⁻
339 (8%), separately. While the simulated PM_{2.5} concentrations under the two cases were
340 quite close. The influence of source profile variation on the simulated PM_{2.5}
341 concentration was not significant, but the influence on the simulation of chemical
342 components in PM_{2.5} could not be ignored.



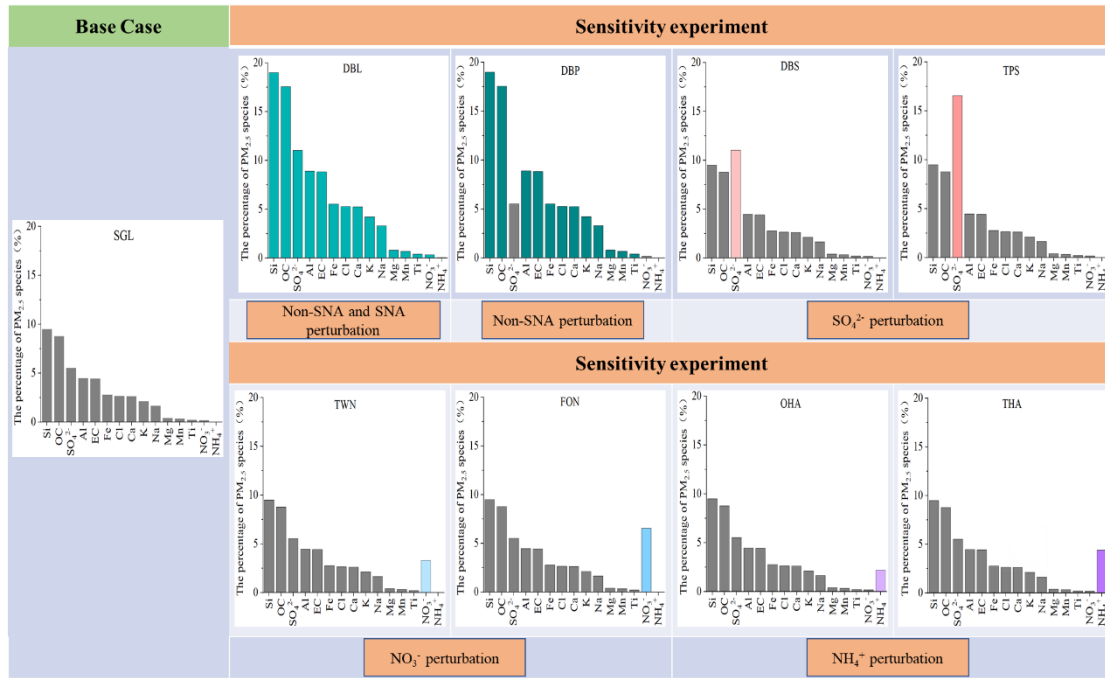
343



344
 345 Fig. 6-3 The percentage relative concentration difference of average simulated concentration result
 346 (PM_{2.5} and its components) between CMAQ_SPE and CAMQ_SPA (relative to CAMQ_SPA)
 347 during simulation period; PM_{2.5} source profiles from SPAPPC and SPECIATE database were
 348 applied in emission inventory for simulating PM_{2.5} and its components used to create speciated
 349 emission inventories for CMAQ, corresponding to case CMAQ_SPA and CMAQ_SPE, respectively.

350 **4 How much did is the variation of source profile adopted in CTMs impact on**
 351 **the simulation of chemical components in PM_{2.5}? How much does it impact?**

352 ~~In order to~~ To quantitatively characterize how much the source profiles affect the
 353 simulation results ~~of PM_{2.5} and its components~~, we selected the chemical composition
 354 of code 000002.5 (Variety of different categories, used for the overall average
 355 composite profiles (Hsu et al., 2019)) in the US EPA Speciate_5.0_0 database ~~as for~~
 356 species allocation of PM_{2.5} components. The corresponding percentages of EC, OC, Mn,
 357 Fe, Ti, Al, Si, Ca, Mg, K, Na, Cl, NH₄⁺, NO₃⁻ and SO₄²⁻ in PM_{2.5} were shown in Fig. 7
 358 4 (SGL, base case simulation).



359

360

361

362

Fig. 7-4 The general roadmap of sensitivity tests (The histogram in each case were the speciation profile in CTMs; SNA represent SO_4^{2-} , NO_3^- , and NH_4^+ , Non-SNA represent other components in $\text{PM}_{2.5}$).

363

Table 1 The content of sensitivity experiment cases

Experiment Cases	Description ³
Case S0 (DBL): add perturbation to Non-SNA and SNA ¹	The percentage of all the listed components in the source profile of base case (SGL) were doubled, and the proportion of unlisted components (Other) ² decreased to 9%.
Case S1 (DBP): add perturbation to Non-SNA	The percentages of non-SNA were doubled and SNA(SO_4^{2-} , NO_3^- , NH_4^+) species stayed the same with that in SGL (the cumulative percentage of listed species was 85.3%), the proportion of unlisted components decreased to 14.7%.
Case S2 (DBS and TPS): add perturbation to SO_4^{2-}	The percentage of SO_4^{2-} was doubled (11%, DBS, represented Double Sulfate), tripled (16.5%, TPS, represented Triple Sulfate) and the other listed 14 species stayed the same with that in SGL (the cumulative percentage of listed species was 51% and 57%, respectively), the proportion of unlisted components decreased to 49% and 43%.
Case S3 (TWN and FON): add perturbation to NO_3^-	The NO_3^- content was raised up to 20 times (3.3%, TWN) and 40 times (6.6%, FON) of that in SGL (0.16%), the other 14 species stayed the same with SGL (the cumulative percentage of listed species was 48.6% and 51.9%, respectively), the proportion of unlisted components decreased to 51.4% and 48.1%.

Case ~~S4~~(OHA and THA):
add perturbation to NH_4^+

The NH_4^+ content was raised up to 100 times (2.2%, OHA), 200 times (4.4%, THA) of that in SGL (0.02%), the other 14 species stayed the same with SGL (the cumulative percentage of listed species was 47.7% and 49.9%, respectively), the proportion of unlisted components decreased to 52.3% and 50.1%.

Note:

1. SNA represent SO_4^{2-} , NO_3^- , and NH_4^+ , Non-SNA represent other components in $\text{PM}_{2.5}$.
2. The listed components contain Al, Ca, Cl, EC, Fe, K, Mg, Mn, Na, OC, Si, Ti, NH_4^+ , NO_3^- and SO_4^{2-} , unlisted components are classified as Other.

3. The source profiles in all cases listed in the table were calculated based on the base case SGL. In the design of simulation cases, the reason why the disturbance amplitude of NH_4^+ and NO_3^- were significantly higher than that of other components such as SO_4^{2-} and Non-SNA, was because the percentages of NH_4^+ and NO_3^- in the base source profile (SGL, based on the chemical composition of code 000002.5 in the EPA Speciate_5.0_0 database) were very low, while the percentage of NH_4^+ and NO_3^- in SPAPPC exhibited in section 2.2 were orders of magnitude higher than those in SGL.

364 Given the large number and complex chemical composition of $\text{PM}_{2.5}$, it is
365 advisable to classify ~~it~~ them reasonably before designing sensitivity experiments. The
366 Case ~~DBLS0~~ was to double the percentage of the listed 15 components mentioned in
367 the above (SGL base case(SGL)) in $\text{PM}_{2.5}$ species allocation for emission sources (DBL
368 case, the cumulative percentage was 91%, the details were are shown in Fig. 4 and Table
369 1). As the percentage of these components increased, the proportion of unlisted
370 components (represented by “Other”) decreased to 9% in order to meet the requirement
371 that the total percentage of all components is 100%. Then we compared the simulation
372 results before (SGL case) and after perturbation (DBL case) in species allocation of
373 $\text{PM}_{2.5}$ sources.

374 In the case DBL, when the percentage of all the components except “other” were
375 doubled in the source profile, the simulated concentrations of Al, Ca, Cl, EC, Fe, K,
376 Mg, Mn, Na, OC, Si and Ti doubled as well, while the simulated concentration of NO_3^- ;
377 and SO_4^{2-} and NH_4^+ only increased at about 3%, 10% and NH_4^+ decreased by 4%,
378 respectively, although the simulated concentration of $\text{PM}_{2.5}$ was not obviously changed
379 (Detailed simulation results were shown in Table S14). ~~Through this Case S0DBL, we~~
380 ~~found that the~~ The simulation test results for SNA (SO_4^{2-} , NO_3^- , and NH_4^+) and Non-
381 SNA were obviously different. Therefore, we divided the components in the source

382 profile into two groups (Non-SNA and SNA) and designed a series of sensitivity tests
 383 listed in next section to further explore how species allocation of PM_{2.5} in emission
 384 sources ~~of CTMs would~~ affect the simulation results. The sketch of sensitivity
 385 experiment design idea is shown in Figure S7.

386 4.1 Sensitivity tests design

387 ~~Based on the Case S0 DBL results, sensitivity~~ Sensitivity tests were designed by
 388 changing the percentages of the target components and related components in the base
 389 case (SGL): add perturbation on each component of Non-SNA, ~~perturbation~~ on SO₄²⁻,
 390 ~~perturbation~~ on NO₃⁻, and ~~perturbation~~ on NH₄⁺. The general roadmap of sensitivity
 391 tests ~~was is~~ shown in Fig. 4, and the illustration of each case was summarized in Table
 392 1. The basic rules must be followed: a) perturbation on the percentage of each
 393 component in source profile fell within the variation range of its measured value
 394 described in section 2.2. b) The sum of the percentage of listed Non-SNA, SNA and
 395 Other components in PM_{2.5} source profile was 100%.

396 4.2 Sensitivity of simulated components to changes in source profile~~Evaluation~~ 397 ~~index for simulation result~~

398 ~~In order to quantify the concentration changes of simulated PM_{2.5} components~~
 399 ~~caused by the perturbation in source profile, we~~ We proposed the sensitivity coefficient
 400 (δ) as evaluation index. The calculation formula is as follows:

$$401 \delta_{i,p} = \frac{\frac{C_{i_case}}{C_{PM_{2.5_case}}} \times 100\% - \frac{C_{i_base}}{C_{PM_{2.5_base}}} \times 100\%}{P_{p_case} - P_{p_base}} \quad (\text{For DBL and DBP, } p = i; \text{For other cases, } p = j)$$

402 (2)

$$403 \delta_i = \begin{cases} \frac{\frac{C_{i_case}}{C_{PM_{2.5_case}}} \times 100\% - \frac{C_{i_base}}{C_{PM_{2.5_base}}} \times 100\%}{P_{i_case} - P_{i_base}} & (\text{For DBL and DBP}) \\ \frac{\frac{C_{i_case}}{C_{PM_{2.5_case}}} \times 100\% - \frac{C_{i_base}}{C_{PM_{2.5_base}}} \times 100\%}{P_{j_case} - P_{j_base}} & (\text{For other cases}) \end{cases} \dots\dots\dots (2)$$

404 Wherein, $\delta_{i,p}$ is the sensitivity coefficient of component i relative to component p,

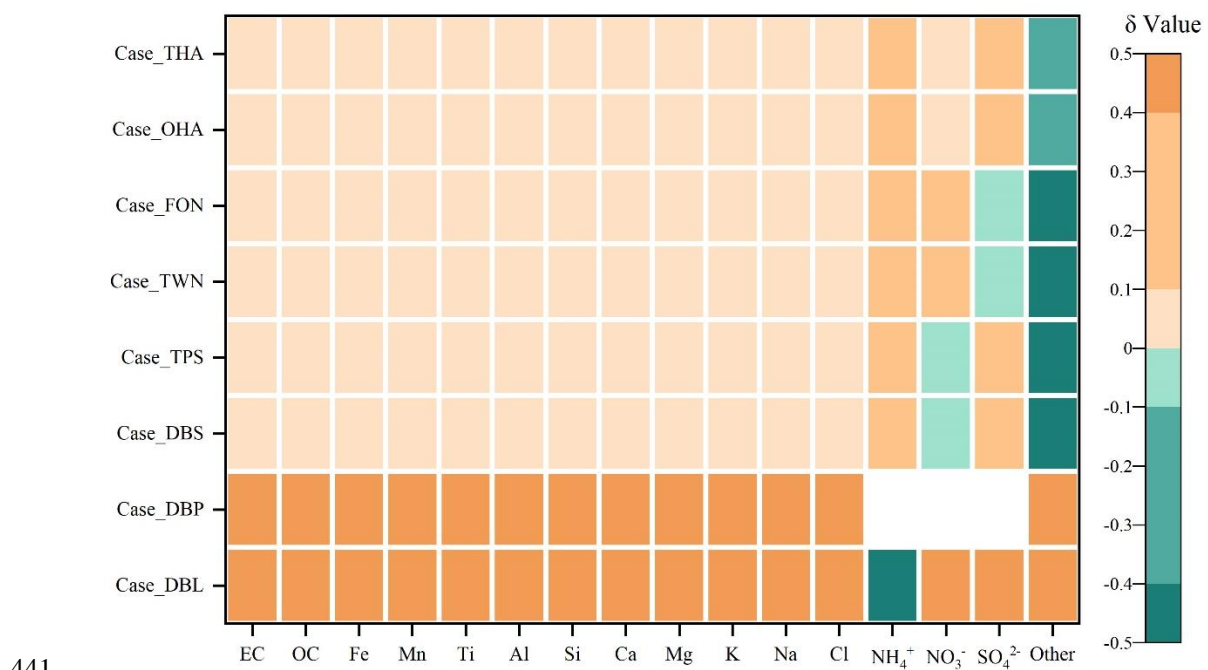
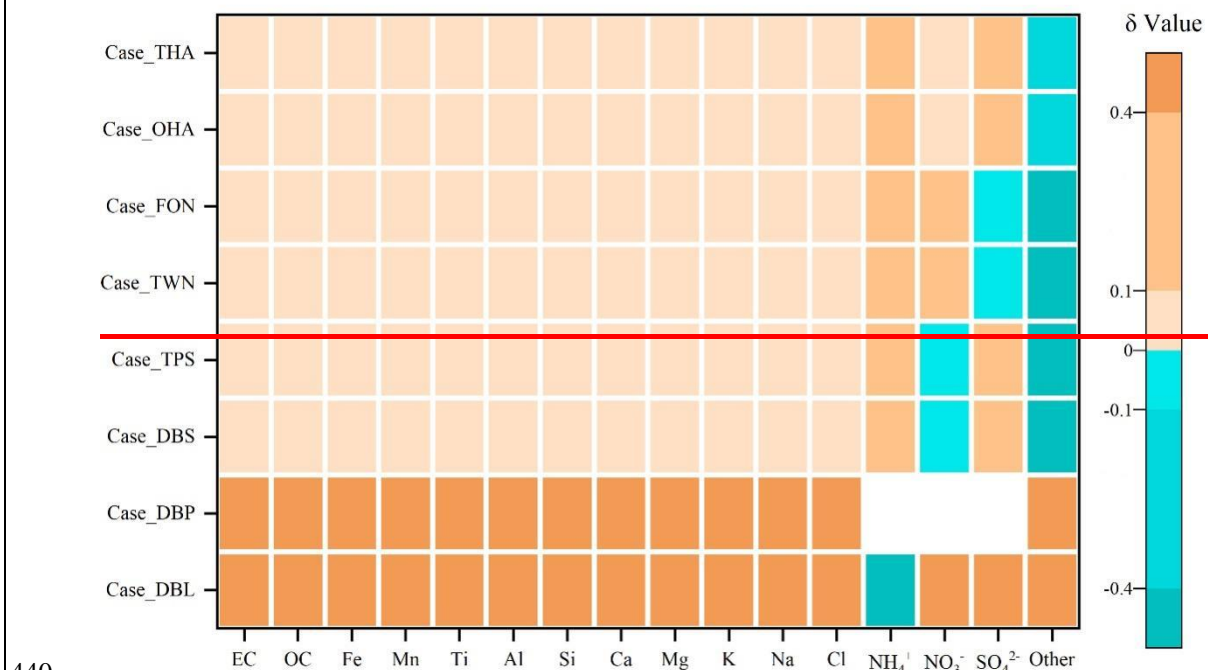
405 representing the change ~~of-in-the~~ simulated value of its content in ambient PM_{2.5}
 406 corresponded to 1% perturbation in the source profiles. C_{i_case} is the simulation result
 407 of component i in ~~different-each~~ sensitivity experiment cases, $\mu\text{g}/\text{m}^3$; C_{i_base} is the
 408 simulation result of components i in base case, $\mu\text{g}/\text{m}^3$; $C_{PM_{2.5}_case}$ is the simulation
 409 result of PM_{2.5} in ~~different-each~~ sensitivity experiment cases, $\mu\text{g}/\text{m}^3$; $C_{PM_{2.5}_base}$ is the
 410 simulation result of PM_{2.5} in base case, $\mu\text{g}/\text{m}^3$; P_{iP_case} is the percentage of component
 411 i in ~~different~~ source profile of sensitivity experiment cases, %; P_{j_case} is the ~~percentage~~
 412 ~~of~~ perturbed component j in different source profile of sensitivity experiment cases, %;
 413 P_{iP_base} is the percentage of component i in ~~base-case~~ source profile of base case, %;
 414 P_{j_base} is the ~~percentage of perturbed component j in base case source profile~~, %.

415 The positive value of δ means the simulated concentration of PM_{2.5} component
 416 increases (decreases) with the increase (decrease) of ~~the~~ perturbation ~~to-on~~ the
 417 percentage of components in source profile, ~~while the meaning of~~ negative δ is just the
 418 opposite. If the absolute value of δ is less than or equal to 0.1, the simulated ~~result of~~
 419 ~~PM_{2.5}-chemical~~ component is considered to be insensitive to the corresponding
 420 variation of source profile; If the absolute value of δ falls between 0.1 and 0.4 (included),
 421 the simulated ~~results of PM_{2.5}-chemical~~ component is considered to be sensitive to the
 422 variation of source profile; If the absolute value of δ is larger than 0.4, the simulated
 423 ~~results of PM_{2.5}-chemical~~ component is very sensitive to the variation of source profile.
 424 The greater the absolute value of δ is, indicates the variation of source profile adopted
 425 in CMAQ has more obvious impact on the simulated results of PM_{2.5} chemical
 426 components.

427 **4.3 The response of simulated PM_{2.5} components**

428 Fig. ~~8-5~~ listed the sensitivity coefficients of simulated ambient PM_{2.5} components
 429 to the perturbation of source profile under each test case. In case DBL (doubled the
 430 percentage of the listed components in the source profile of base case and decreased the
 431 proportion of unlisted other components to 9%-), ~~-(The percentage of all the listed~~
 432 ~~components in the source profile of base case (SGL) was doubled)~~, the sensitivity

433 coefficient (δ) of NH_4^+ was negative, and the absolute value was ~~the highest~~, indicating
 434 that the simulated proportion of NH_4^+ in ambient $\text{PM}_{2.5}$ decreased, and it was very
 435 sensitive to the variation of source profile. Conversely, the sensitivity coefficient of
 436 NO_3^- was close to 1, which illustrated that the simulated proportion of NO_3^- in ambient
 437 $\text{PM}_{2.5}$ increased proportionally with the change in source profile. The simulated ~~δ -of~~
 438 SO_4^{2-} also showed a very sensitive property. The simulated Non-SNA concentrations
 439 were doubled when compared to the base case (SGL).



442 Fig. 8-5 The sensitivity coefficients (δ) of simulated components to the perturbation of adopted
443 source profile in different cases. Note: Each small color box in the figure represented the sensitivity
444 level (indicated by the legend on the right) of $\text{PM}_{2.5}$ components (the x-coordinate) in different cases
445 (y-coordinate). The blank grids in DBP case indicated no perturbation to SNA in $\text{PM}_{2.5}$ source profile
446 under this case.

447 In case DBP, when the percentages of listed Non-SNA (Al, Ca, Cl, EC, Fe, K, Mg,
448 Mn, Na, OC, Si and Ti) in the source profile were doubled, the simulated proportions
449 of Non-SNA (~~Al, Ca, Cl, EC, Fe, K, Mg, Mn, Na, OC, Si and Ti~~) in ambient $\text{PM}_{2.5}$
450 synchronous increased, and were very sensitive to the change in the adopted source
451 profile with a sensitivity coefficient (δ) of 0.5. Interestingly, the simulated concentration
452 of SNA in ambient $\text{PM}_{2.5}$ also changed although the SNA in source profile did not
453 change, the concentration of NO_3^- and SO_4^{2-} increased by 2% and 3%, respectively,
454 NH_4^+ decreased by 10% (Detail simulation results of different each cases were shown
455 on Table S15~S21).

456 Under SO_4^{2-} perturbation cases (Case DBS and Case TPS), we found the simulated
457 results of Non-SNA and NO_3^- had no obvious variation ~~when~~ compared with the base
458 case. Either in Case DBS or in Case TPS, the δ of Non-SNA and NO_3^- were always
459 between -0.1 to 0.1. But when the percentage of SO_4^{2-} was doubled in ~~$\text{PM}_{2.5}$~~ -source
460 profile (DBS), the simulated concentration of NH_4^+ and SO_4^{2-} increased by 6% and 8%,
461 respectively. In Case TPS (the percentage of SO_4^{2-} was tripled), the simulated
462 concentration of NH_4^+ and SO_4^{2-} were increased by 11% and 16%, respectively. The δ
463 of NH_4^+ and SO_4^{2-} were 0.12 and 0.36, sensitive toward to positive direction with the
464 increase of SO_4^{2-} in the source profile.

465 In the situation of NO_3^- perturbation in source profile (Case TWN and Case FON),
466 the simulated ~~concentrations of~~ Non-SNA hardly change when compared to the base
467 case, while ~~the~~ changing characteristics patterns of simulated SNA ~~concentrations~~ were
468 different. ~~In cases TWN and FON, the~~ The simulation concentration of NH_4^+ increased
469 by 2.6% and 5.4% ~~when~~ compared with the base case, the simulated NO_3^- increased by
470 14% and 30%, the simulated SO_4^{2-} decreased slightly, even could be neglected in some
471 observation sites. The simulated concentrations of Non-SNA and SO_4^{2-} were insensitive
472 to the perturbation of NO_3^- in ~~$\text{PM}_{2.5}$~~ -source profile; NH_4^+ was sensitive, and NO_3^- was

473 very sensitive.

474 When we put perturbation ~~to~~ on NH_4^+ in the source profile (Case OHA and Case
475 THA), the simulation results of Non-SNA were almost not changed, the simulated
476 concentration of SO_4^{2-} , NH_4^+ , NO_3^- increased ~~in OHA and THA~~. The δ of SNA to the
477 variation of NH_4^+ in the source profile were positive and $\delta_{\text{SO}_4^{2-}, \text{NH}_4^+}(\text{SO}_4^{2-}) > \delta_{\text{NH}_4^+, \text{NH}_4^+}$
478 $\delta(\text{NH}_4^+) > \delta_{\text{NO}_3^-, \text{NH}_4^+}(\text{NO}_3^-)$, SO_4^{2-} and NH_4^+ were sensitive to the NH_4^+ perturbation in
479 the source profile, but NO_3^- was not so sensitive.

480 In general, the simulation results of components in ambient $\text{PM}_{2.5}$ were affected in
481 one way or another by the change of source profiles adopted by CMAQ. Both of the
482 simulated Non-SNA and SNA were very sensitive to the perturbation of Non-SNA in
483 source profile. When the percentage of SNA changed in the source profile, simulated
484 ~~concentrations of~~ Non-SNA generally have little change, but the simulation results of
485 SNA could change in different levels/patterns: the simulated SO_4^{2-} was very sensitive
486 and NH_4^+ was sensitive to the perturbation of SO_4^{2-} in source profile; ~~;~~ simulated NO_3^-
487 was very sensitive and NH_4^+ was sensitive to the perturbation of NO_3^- in source profile;
488 ~~;~~ SO_4^{2-} and NH_4^+ were sensitive to the perturbation of NH_4^+ in source profile. The
489 simulated component such as SO_4^{2-} was influenced not only by the change of SO_4^{2-}
490 itself but also by other components like some Non-SNA and NH_4^+ in the source profile.
491 In other words, there was a linkage effect, variation of some components in the source
492 profile would bring changes to the simulated results of other components.

493 **5 How does the variation of source profile adopted in CTMs impact on the** 494 **simulation of chemical components in $\text{PM}_{2.5}$? How does the impact work?**

495 The variation of species allocation in emission sources can directly affected the
496 composition of aerosol system in CTMs. In CMAQv5.0.2, the aerosol thermodynamic
497 equilibrium process ~~was~~ is carried out according to ISORROPIA II, including a SO_4^{2-} -
498 NO_3^- - Cl^- - NH_4^+ - Na^+ - K^+ - Mg^{2+} - Ca^{2+} - H_2O system ~~which was established on the basis of~~
499 ~~ISORROPIA I by adding the effects of K^+ , Ca^{2+} and Mg^{2+}~~ (Detailed equilibrium
500 relations were shown in Table S22). Some assumptions had been made in the

501 ISORROPIA model to simplify the simulation system (Fountoukis and Nenes, 2007):
 502 (1) Because the vapor pressure of sulfuric acid and metal salts (such as Na⁺, Ca²⁺, K⁺,
 503 Mg²⁺) were very low, it was assumed that all the sulfuric acid and metal salts in the
 504 system existed in the aerosol phase; (2) For ammonia in the system, it was preferred to
 505 have an irreversible reaction with sulfuric acid to produce ammonium sulfate. Only
 506 when there was still surplus NH₃ after the neutralization of H₂SO₄, can it have a
 507 reversible reaction with HNO₃ and HCl to produce NH₄NO₃ and NH₄Cl. (3) For sulfuric
 508 acid in the system, if there were metal ions (such as Ca²⁺, Mg²⁺, K⁺, Na⁺) in the system,
 509 sulfuric acid would react with metal ions to produce metal salts. Only in the case of
 510 insufficient sodium, sulfuric acid would react with ammonia. Based on these
 511 assumptions, the ISORROPIA model introduced the following three judgment
 512 parameters (R₁, R₂ and R₃ ~~were calculated by the following formulas~~) to determine the
 513 simulation subsystems, these parameters are calculated by the following formulas:

$$514 \quad R_1 = \frac{[\text{NH}_4^+] + [\text{Ca}^{2+}] + [\text{K}^+] + [\text{Mg}^{2+}] + [\text{Na}^+]}{[\text{SO}_4^{2-}]} \dots\dots\dots (3)$$

$$515 \quad R_2 = \frac{[\text{Ca}^{2+}] + [\text{K}^+] + [\text{Mg}^{2+}] + [\text{Na}^+]}{[\text{SO}_4^{2-}]} \dots\dots\dots (4)$$

$$516 \quad R_3 = \frac{[\text{Ca}^{2+}] + [\text{K}^+] + [\text{Mg}^{2+}]}{[\text{SO}_4^{2-}]} \dots\dots\dots (5)$$

517 Where [X] denotes molar concentration of component (mol·m⁻³), R₁, R₂ and R₃
 518 are termed as “total sulfate ratio”, “crustal species and sodium ratio” and “crustal
 519 species ratio” respectively; The number of species and equilibrium reactions are
 520 determined by the relative abundance of NH₃, Na, Ca, K, Mg, HNO₃, HCl, H₂SO₄, as
 521 well as the ambient relative humidity and temperature. Guided by the value of R₁, R₂
 522 and R₃, 5 aerosol composition regimes in ISORROPIA are defined. (Detail rules are
 523 shown in Table S27).

524 In this paper, R₁, R₂, R₃ and the ~~potential aerosol species~~~~corresponding solid phase~~
 525 ~~species~~-under ~~different each perturbation~~-sensitivity test cases on source profiles-were
 526 shown in Table 2. These components achieved thermodynamic equilibrium in the order

527 of preference for more stable salts, obviously, the simulation processes of these
 528 components may influence each other.

529
$$R_1 = \frac{[\text{NH}_4^+] + [\text{Ca}^{2+}] + [\text{K}^+] + [\text{Mg}^{2+}] + [\text{Na}^+]}{[\text{SO}_4^{2-}]} \dots\dots\dots (3)$$

530
$$R_2 = \frac{[\text{Ca}^{2+}] + [\text{K}^+] + [\text{Mg}^{2+}] + [\text{Na}^+]}{[\text{SO}_4^{2-}]} \dots\dots\dots (4)$$

531
$$R_3 = \frac{[\text{Ca}^{2+}] + [\text{K}^+] + [\text{Mg}^{2+}]}{[\text{SO}_4^{2-}]} \dots\dots\dots (5)$$

532

Table 2 Potential aerosol species in ISORROPIA II under different cases

Cases	R ₁	R ₂	R ₃	Solid phase species*
SGL, DBL TWN, FON	2.53	2.52	1.9	CaSO₄, MgSO₄, K₂SO₄, Na₂SO₄, NaCl, NaNO₃, NH₄Cl, NH₄NO₃
DBS	1.26	1.26	0.95	CaSO ₄ , MgSO ₄ , K ₂ SO ₄ , KHSO ₄ , Na ₂ SO ₄ , NaHSO ₄ , (NH ₄) ₂ SO ₄ , NH ₄ HSO ₄ , (NH ₄) ₃ H(SO ₄) ₂
TPS	0.84	0.84	0.63	CaSO ₄ , KHSO ₄ , NaHSO ₄ , NH ₄ HSO ₄
DBP	5.04	5.03	3.79	CaSO ₄ , MgSO ₄ , K ₂ SO ₄ , CaCl ₂ , Ca(NO ₃) ₂ , MgCl ₂ ,
OHA	3.58	2.52	2.95	Mg(NO ₃) ₂ , KCl, KNO ₃ , NaCl, NaNO ₃ , NH ₄ Cl,
THA	4.64	2.52	4.02	NH ₄ NO ₃

533 * The solid phase species were determined based on the research of (Fountoukis and Nenes, 2007)

534

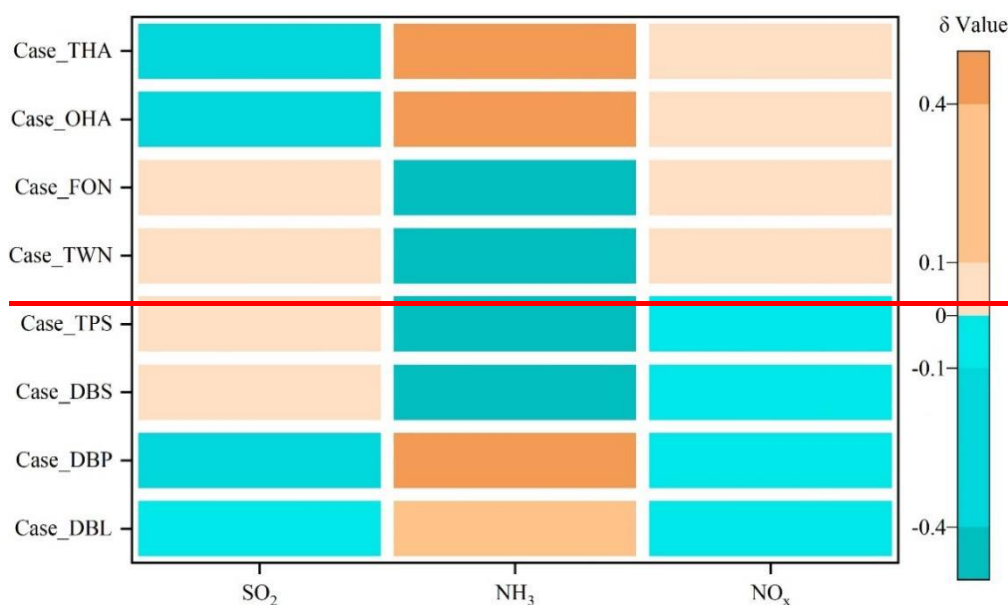
Table 2 Potential aerosol species in ISORROPIA II under different cases

Cases	R ₁	R ₂	R ₃	Solid phase species*
<u>SGL</u>	<u>2.53</u>	<u>2.52</u>	<u>1.9</u>	<u>CaSO₄, MgSO₄, K₂SO₄, Na₂SO₄, NaCl, NaNO₃, NH₄Cl, NH₄NO₃</u>
<u>DBL</u>	<u>2.53</u>	<u>2.52</u>	<u>1.9</u>	<u>CaSO₄, MgSO₄, K₂SO₄, Na₂SO₄, NaCl, NaNO₃, NH₄Cl, NH₄NO₃</u>
<u>DBP</u>	<u>5.04</u>	<u>5.03</u>	<u>3.79</u>	<u>CaSO₄, MgSO₄, K₂SO₄, CaCl₂, Ca(NO₃)₂, MgCl₂, Mg(NO₃)₂, KCl, KNO₃, NaCl, NaNO₃, NH₄Cl, NH₄NO₃</u>
<u>DBS</u>	<u>1.26</u>	<u>1.26</u>	<u>0.95</u>	<u>CaSO₄, MgSO₄, K₂SO₄, KHSO₄, Na₂SO₄, NaHSO₄, (NH₄)₂SO₄, NH₄HSO₄, (NH₄)₃H(SO₄)₂</u>
<u>TPS</u>	<u>0.84</u>	<u>0.84</u>	<u>0.63</u>	<u>CaSO₄, KHSO₄, NaHSO₄, NH₄HSO₄</u>
<u>TWN</u>	<u>2.53</u>	<u>2.52</u>	<u>1.9</u>	<u>CaSO₄, MgSO₄, K₂SO₄, Na₂SO₄, NaCl, NaNO₃, NH₄Cl, NH₄NO₃</u>
<u>FON</u>	<u>2.53</u>	<u>2.52</u>	<u>1.9</u>	<u>CaSO₄, MgSO₄, K₂SO₄, Na₂SO₄, NaCl, NaNO₃, NH₄Cl, NH₄NO₃</u>
<u>OHA</u>	<u>3.58</u>	<u>2.52</u>	<u>2.95</u>	<u>CaSO₄, MgSO₄, K₂SO₄, CaCl₂, Ca(NO₃)₂, MgCl₂, Mg(NO₃)₂, KCl, KNO₃, NaCl, NaNO₃, NH₄Cl,</u>

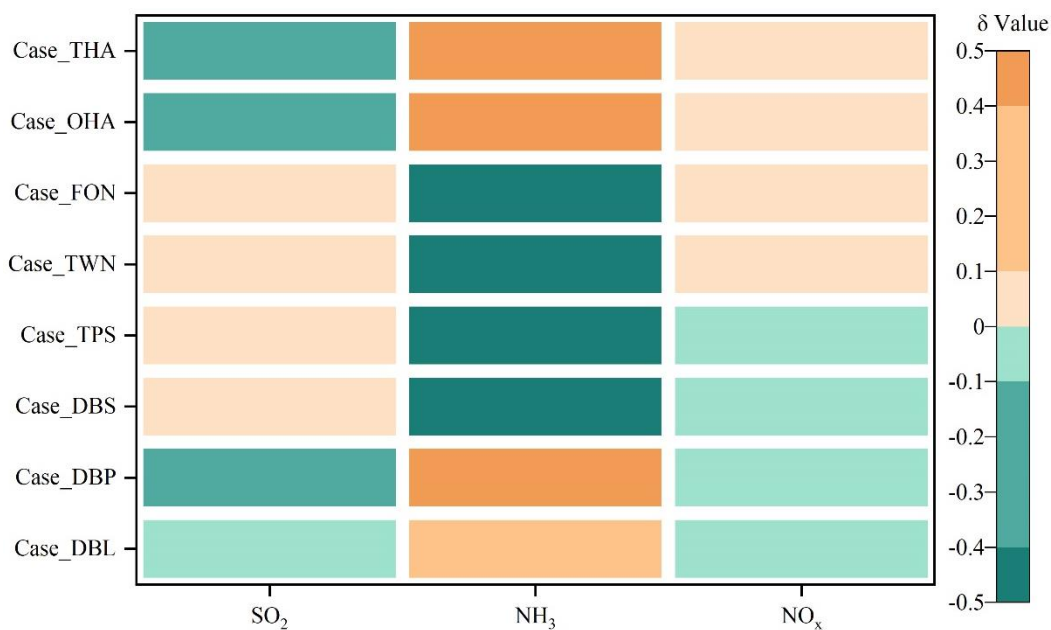
				<u>NH₄NO₃</u>
				<u>CaSO₄, MgSO₄, K₂SO₄, CaCl₂, Ca(NO₃)₂, MgCl₂,</u>
<u>THA</u>	<u>4.64</u>	<u>2.52</u>	<u>4.02</u>	<u>Mg(NO₃)₂, KCl, KNO₃, NaCl, NaNO₃, NH₄Cl,</u>
				<u>NH₄NO₃</u>

535 * The solid phase species were determined based on the research of (Fountoukis and Nenes, 2007)

536 In Non-SNA perturbation case, when the percentage of Non-SNA in source profile
 537 doubled (Case DBP), meant there were more Na, K, Mg, Ca, Cl participated in aerosol
 538 chemistry, the model system needed more SO₄²⁻ and NO₃⁻ on the basis of charge balance
 539 and the thermodynamic equilibrium shifted to the direction of consuming Ca Mg, K
 540 and Na, which resulted in the increase of the simulated concentration of SO₄²⁻ and NO₃⁻.
 541 Meanwhile, according to the rule of anions preferentially binding with nonvolatile
 542 cations in ISORROPIA, the increased cations Na⁺, K⁺, Mg²⁺, Ca²⁺ directly led to
 543 the decrease of anions binding with NH₄⁺, there were less reaction dose between SO₄²⁻
 544 and NH₄⁺ to form (NH₄)₂SO₄ or NH₄HSO₄, ultimately resulted in a decrease in
 545 simulated concentration of NH₄⁺ ~~when compared to~~ with the base case. Because in this
 546 case more anions such as SO₄²⁻ were passively needed, according to the principle of
 547 chemical equilibrium mentioned above, the chemical conversion of SO₂ to SO₄²⁻ was
 548 promoted, the simulated secondary SO₄²⁻ increased, this could be proved by that the
 549 sensitivity coefficient δ of SO₂ in Case DBP was negative (shown in Fig. 96, details of
 550 other monitoring stations were shown Table S24).



551



552
553 Fig.9-6 The sensitivity coefficients (δ) of simulated gas pollutants to the change of adopted source
554 profile in different cases.

555 Similarly, with the increase of metal ions in the system to bond with anions, the
556 number of anions which can bind to NH_4^+ decreased. The system needed less NH_4^+ and
557 weakened the need for conversion from NH_3 to NH_4^+ , the simulated NH_4^+ concentration
558 decreased while the δ of NH_3 was positive and very sensitive. Different trends of
559 simulated concentration of gaseous pollutants mirrored the rules mentioned above from
560 another aspect. The δ of SO_2 and NO_x was negative, NH_3 was positive. We could see
561 the same phenomena in DBL case (Fig. 96). When the percentages of Non-SNA in
562 source profile increased, they not only affected the simulated concentration of Non-
563 SNA, but also the secondary SO_4^{2-} , NO_3^- and NH_4^+ .

564 In SO_4^{2-} perturbation cases (Case DBS and TPS), as the percentage of SO_4^{2-} in
565 source profile increased, for the chemical reactions of sulfate radical consuming (as
566 shown in Table S22), the chemical equilibrium would move toward the products ~~when~~
567 compared ~~to~~-with the base case. While for the chemical reactions of sulfate radical
568 formation (The equations were shown in Table S23), meant the product was added in,
569 the chemical equilibrium would be pushed toward the reactants. The chemical reactions
570 between SO_4^{2-} and NH_4^+ would shift to the direction of $(\text{NH}_4)_2\text{SO}_4$ generation, we could
571 see the simulated concentrations of NH_4^+ in DBS and TPS were both higher and NH_3

572 were lower than those in the base case (SGL). In addition, when more SO_4^{2-} was added
573 in the system, the conversion of SO_2 to SO_4^{2-} was affected in some level and consumed
574 less SO_2 than the base case, simulated SO_2 showed insensitive but positive trend (Fig.9).
575 And ~~from~~ the potential solid phase species in ISORROPIA II under DBS and TPS cases
576 (shown in Table 32), ~~the solid phase species~~ were mainly consisted of sulfate salts, so
577 the simulated concentration of NO_3^- did not change apparently.

578 As the percentage of NO_3^- in source profile increased (Case FON and TWN), the
579 associated chemical equilibrium shifted towards the consumption of NO_3^- , such as NH_4^+
580 + $\text{NO}_3^- \rightarrow \text{NH}_4\text{NO}_3$, which would also consume more NH_4^+ and form more ammonium
581 salt, finally consumed more NH_3 because of $\text{NH}_3(\text{gas}) + \text{H}_2\text{O}(\text{aq}) \rightarrow \text{NH}_4^+(\text{aq}) + \text{OH}^-$
582 (aq). The simulation results also manifested that the concentration of NH_4^+ increased
583 while that of NH_3 decreased. Based on the assumption of ISORROPIA, the cations like
584 Na^+ , K^+ , Mg^{2+} , Ca^{2+} and NH_4^+ preferentially to react with SO_4^{2-} , only if there were
585 cations left after neutralized SO_4^{2-} , could they react with NO_3^- to form salts, so the
586 simulated concentration of SO_4^{2-} was not obviously changed. Accordingly, the
587 simulated concentration of NO_x and SO_2 almost unchanged (The δ of NO_x and SO_2 ~~was~~
588 displayed insensitive).

589 In the cases of NH_4^+ perturbation (Case OHA and THA), when the percentage of
590 NH_4^+ in source profile increased, the related chemical equilibrium shifted towards the
591 direction of NH_4^+ consumption, such as in $2\text{NH}_4^+ + \text{SO}_4^{2-} \rightarrow (\text{NH}_4)_2\text{SO}_4$, more SO_4^{2-}
592 was consumed at the same time, which further promoted the conversion of SO_2 to SO_4^{2-} .
593 The increased NH_4^+ in OHA and THA also would inhibit the conversion of NH_3 to NH_4^+
594 ~~when compared to~~ with the base case. This, in turn appeared as the increase of the
595 simulated secondary SO_4^{2-} and NH_3 , and the decrease of the simulated SO_2 .

596 In summary, the effects of source profile variation on the simulation results of
597 different components were linked. When the percentages of Non-SNA, SO_4^{2-} , NO_3^- and
598 NH_4^+ in the source profile changed, they not only affected the simulated concentration
599 of themselves, but also affected the simulation results of some other components. Both
600 the simulation results of primary components and secondary components were affected

601 by the change of source profile, the secondary SO_4^{2-} and NH_4^+ were affected more than
602 the secondary NO_3^- .

603 6 Conclusions

604 ~~Although the influence of source profile variation on the simulated concentration~~
605 ~~of ambient $\text{PM}_{2.5}$ is not significant, its influence on the simulated chemical $\text{PM}_{2.5}$~~
606 ~~components cannot be ignored. The variation of simulated components ranges from~~
607 ~~8% to 167% under selected different source profiles, and as the simulation results of~~
608 ~~some components are sensitive to the adopted $\text{PM}_{2.5}$ -source profile in CTMs, e.g., both~~
609 ~~the simulated Non-SNA and SNA are sensitive to the perturbation of Non-SNA in~~
610 ~~source profile, the simulated SO_4^{2-} and NH_4^+ are sensitive to the perturbation of SO_4^{2-} ,~~
611 ~~simulated NO_3^- and NH_4^+ are sensitive to the perturbation of NO_3^- , SO_4^{2-} and NH_4^+ are~~
612 ~~sensitive to the perturbation of NH_4^+ . These influences are not only specific to an~~
613 ~~individual component, but also can be transmitted and linked among components, that~~
614 ~~is, the influence path is connected to chemical mechanisms in the model since the~~
615 ~~variation of species allocation in emission sources directly affect the thermodynamic~~
616 ~~equilibrium system (ISORROPIA II, SO_4^{2-} - NO_3^- - Cl^- - NH_4^+ - Na^+ - K^+ - Mg^{2+} - Ca^{2+} - H_2O~~
617 ~~system).~~

618 ~~It is generally believed that changes in source profile would have an impact on the~~
619 ~~simulation result of primary $\text{PM}_{2.5}$. Traditionally, the source profiles are regarded as a~~
620 ~~primary emission, but interestingly, the simulation of secondary components could be~~
621 ~~affected as well. their variation could affect the simulation result of secondary~~
622 ~~components as well in CTMs. We found the perturbation of $\text{PM}_{2.5}$ source profile caused~~
623 ~~the variation of simulation results of gaseous pollutantssimulated gaseous pollutants,~~
624 ~~and related by influencing related chemical reactions like gas-phase chemistry of SO_2 ,~~
625 ~~NO_x and NH_3 , which mirrored that the perturbation of source profile had an effect on~~
626 ~~the simulation of secondary $\text{PM}_{2.5}$ components. Overall, the emission source profile~~
627 ~~used in CTMs is one of the important factors affecting the simulation results of $\text{PM}_{2.5}$~~
628 ~~chemical components. Additionally, organic species are one of the most important~~

629 components in PM_{2.5} and gain much more attention on human health. While the number
630 of organic species in source profile is relatively scarce which brings a challenge for
631 simulation test designing, the influence of source profile on the simulation results of
632 ~~the variation of source profile adopted in CTMs has an impact on the simulation of~~
633 organic species is not taken into account in this study.

634 With the change of fuel and raw materials, the development of production
635 technology and the innovation of pollution treatment technology in recent years, some
636 components have changed significantly in ~~the~~ source profiles. Given the important role
637 of air quality simulation in decision making for pollution control environment
638 ~~management~~ and health risk assessment, the representativeness and timeliness of the
639 source profile should be considered.

640 Our study tentatively discussed the influence~~impact~~ mechanism of PM_{2.5} emission
641 source profiles on the simulation results of PM_{2.5}-components ~~simulation results~~ in
642 CTMs. ~~In the next work, we will use different source profile for simulation, compare~~
643 ~~the simulation results with local measured PM_{2.5} components and discuss the influence~~
644 ~~of sub-source profiles variation on the simulation results. In addition, the~~ The size
645 distribution, mixing state, aging and solubility for different aerosol components might
646 have something to do with source profile, how much the influence of source profile
647 changes on the simulation of these physical and chemical process, is deserved to do in
648 the future.

649 **Data availability**

650 The input datasets for WRF simulation are available at
651 <https://rda.ucar.edu/datasets/ds351.0/index.html> (The National Center for Atmospheric
652 Research (NCAR)). The Multi-resolution Emission Inventory for China (MEICv1.3) is
653 available at http://meicmodel.org/?page_id=135. The PM_{2.5} emission source profiles
654 from database of Source Profiles of Air Pollution (SPAP)
655 (<http://www.nkspap.com:9091/>, Nankai university), SPECIATE database
656 (<https://www.epa.gov/air-emissions-modeling/speciate>, U.S. Environmental Protection

657 Agency's (EPA)), Mendeley data repository (<https://doi.org/10.17632/x8dfshjt9j.2>, Bi
658 et al., 2019).

659 **Code availability**

660 The source code for CMAQ version 5.0.2 is available at
661 <https://github.com/USEPA/CMAQ/tree/5.0.2> (last access: April 2014)
662 (<https://doi.org/10.5281/zenodo.1079898>, US EPA Office of Research and
663 Development, 2018). The source code for WRF version 3.7.1 is available at
664 <https://www2.mmm.ucar.edu/wrf/src/WRFV3.7.1.TAR.gz>.

665 **Author contributions**

666 Zhongwei Luo: Data curation and collection, writing—original draft. Yan Han:
667 Modeling, writing—original draft. Kun Hua: Data collection. Yufen Zhang:
668 Supervision—Review & editing. Jianhui Wu: Supervision in source profile. Xiaohui Bi:
669 Supervision in source profile. Qili Dai: Resources. Baoshuang Liu: Resources. Yang
670 Chen: Modification and editing. Xin Long: Supervision in modeling. Yinchang Feng:
671 Supervision—Review & editing.

672 **Competing interests**

673 The authors declare that they have no known competing financial interests or
674 personal relationships that could have appeared to influence the work reported in this
675 paper.

676 **Disclaimer. Publisher's note**

677 Copernicus Publications remains neutral with regard to jurisdictional claims in
678 published maps and institutional affiliations.

679 **Acknowledgements**

680 We would like to thank the National Natural Science Foundation of China (grant
681 number 42177465) for providing funding for the project. We are grateful for the
682 Inventory Spatial Allocate Tool (ISAT) provided by Kun Wang from Department of Air

683 Pollution Control, Institute of Urban Safety and Environmental Science, Beijing
684 Academy of Science and Technology. We thank two anonymous referees ~~and~~, Astrid
685 Kerkweg (Executive Editor) and Klaus Klingmüller (Top Editor) for helpful
686 discussion the time and effort spent in reviewing the manuscript.

687 **Financial support**

688 This study was financially supported by the National Natural Science Foundation
689 of China (grant number 42177465).

690 **Reference**

- 691 Appel, K. W., Poulou, G. A., Simon, H., Sarwar, G., Pye, H. O. T., Napelenok, S. L., Akhtar, F., Roselle,
692 S. J.: Evaluation of dust and trace metal estimates from the Community Multiscale Air Quality
693 (CMAQ) model version 5.0, *Geosci. Model Dev.*, 6, 883-899, [https://doi.org/10.5194/gmd-6-883-](https://doi.org/10.5194/gmd-6-883-2013)
694 [2013](https://doi.org/10.5194/gmd-6-883-2013), 2013.
- 695 Bi, X., Dai, Q., Wu, J., Zhang, Q., Zhang, W., Luo, R., Cheng, Y., Zhang, J., Wang, L., Yu, Z., Zhang, Y.,
696 Tian, Y., Feng, Y.: Characteristics of the main primary source profiles of particulate matter across
697 China from 1987 to 2017, *Atmos. Chem. Phys.*, 19, 3223-3243, [https://doi.org/10.5194/acp-19-](https://doi.org/10.5194/acp-19-3223-2019)
698 [3223-2019](https://doi.org/10.5194/acp-19-3223-2019), 2019.
- 699 Cao, J., Qiu, X., Gao, J., Wang, F., Wang, J., Wu, J., Peng, L.: Significant decrease in SO₂ emission and
700 enhanced atmospheric oxidation trigger changes in sulfate formation pathways in China during
701 2008–2016, *J. Clean. Prod.*, 326, 129396, <https://doi.org/10.1016/j.jclepro.2021.129396>, 2021.
- 702 Chapel Hill, N.: Operational Guidance for the Community Multiscale Air Quality (CMAQ) Modeling
703 System Version 5.0,
704 [https://www.airqualitymodeling.org/index.php/CMAQ_version_5.0_\(February_2010_release\)_OG](https://www.airqualitymodeling.org/index.php/CMAQ_version_5.0_(February_2010_release)_OG_D#Aerosol_Module)
705 [D#Aerosol_Module](https://www.airqualitymodeling.org/index.php/CMAQ_version_5.0_(February_2010_release)_OG_D#Aerosol_Module), last access: February 2012.
- 706 Chen, Z., Chen, D., Zhao, C., Kwan, M., Cai, J., Zhuang, Y., Zhao, B., Wang, X., Chen, B., Yang, J., Li,
707 R., He, B., Gao, B., Wang, K., Xu, B.: Influence of meteorological conditions on PM_{2.5}
708 concentrations across China: A review of methodology and mechanism, *Environ. Int.*, 139, 105558,
709 <https://doi.org/10.1016/j.envint.2020.105558>, 2020.
- 710 Cheng, N. L., Meng, F., Wang, J. K., Chen, Y. B., Wei, X., Han, H.: Numerical simulation of the spatial
711 distribution and deposition of PM_{2.5} in East China coastal area in 2010 (In Chinese), *Journ. Safety*
712 *Environ.*, 15, 305-310, <https://doi.org/10.13637/j.issn.1009-6094.2015.06.063>, 2015.
- 713 Foley, K. M., Roselle, S. J., Appel, K. W., Bhawe, P. V., Pleim, J., Otte, T., Mathur, R., Sarwar, G., Young,
714 J. O., Gilliam, R.: Incremental testing of the community multiscale air quality (CMAQ) modeling
715 system version 4.7, *Geosci. Model Dev.*, 3, 205-226, <https://doi.org/10.5194/gmd-3-205-2010>, 2010.
- 716 Fountoukis, C., Nenes, A.: ISORROPIA II: a computationally efficient thermodynamic equilibrium
717 model for K⁺-Ca²⁺-Mg²⁺-NH₄⁺-Na⁺-SO₄²⁻-NO₃⁻-Cl⁻-H₂O aerosols, *Atmos. Chem. Phys.*, 7,
718 4639-4659, <https://doi.org/10.5194/acp-7-4639-2007>, 2007.
- 719 Fu, X., Wang, S., Zhao, B., Xing, J., Cheng, Z., Liu, H., Hao, J.: Emission inventory of primary pollutants
720 and chemical speciation in 2010 for the Yangtze River Delta region, China, *Atmos. Environ.*, 70,

721 39-50, <https://doi.org/10.1016/j.atmosenv.2012.12.034>, 2013.

722 Fu, X., Wang, S. X., Chang, X., Cai, S., Xing, J., Hao, J. M.: Modeling analysis of secondary inorganic
723 aerosols over China: pollution characteristics, and meteorological and dust impacts, *Sci. Rep.*, 6,
724 35992, <https://doi.org/10.1038/srep35992>, 2016.

725 Gao, S., Zhang, S., Che, X., Ma, Y., Chen, X., Duan, Y., Fu, Q., Wang, S., Zhou, B., Wei, C., Jiao, Z.:
726 New understanding of source profiles: Example of the coating industry, *J. Clean. Prod.*, 357, 132025,
727 <https://doi.org/10.1016/j.jclepro.2022.132025>, 2022.

728 Guo, R., Yang, J., Liu, Z.: Influence of heat treatment conditions on release of chlorine from Datong coal,
729 *J. Anal. Appl. Pyrol.*, 71, 179-186, [https://doi.org/10.1016/S0165-2370\(03\)00086-X](https://doi.org/10.1016/S0165-2370(03)00086-X), 2004.

730 Guo, Y. Y., Gao, X., Zhu, T. Y., Luo, L., Zheng, Y.: Chemical profiles of PM emitted from the iron and
731 steel industry in northern China, *Atmos. Environ.*, 150, 187-197,
732 <https://doi.org/10.1016/j.atmosenv.2016.11.055>, 2017.

733 Guo, Z., Hao, Y., Tian, H., Bai, X., Wu, B., Liu, S., Luo, L., Liu, W., Zhao, S., Lin, S., Lv, Y., Yang, J.,
734 Xiao, Y.: Field measurements on emission characteristics, chemical profiles, and emission factors
735 of size-segregated PM from cement plants in China, *Sci. Total Environ.*, 151822,
736 <https://doi.org/10.1016/j.scitotenv.2021.151822>, 2021.

737 Han, Y., Xu, H., Bi, X. H., Lin, F. M., Li, J., Zhang, Y. F., Feng, Y. C.: The effect of atmospheric
738 particulates on the rainwater chemistry in the Yangtze River Delta, China, *J. Air Waste Manage.*, 69,
739 1452-1466, <https://doi.org/10.1080/10962247.2019.1674750>, 2019.

740 Hopke, P. K., Dai, Q., Li, L., Feng, Y.: Global review of recent source apportionments for airborne
741 particulate matter, *Sci. Total Environ.*, 740, 140091,
742 <https://doi.org/10.1016/j.scitotenv.2020.140091>, 2020.

743 Hopke, P. K., Feng, Y. C., Dai, Q.: Source apportionment of particle number concentrations: A global
744 review, *Sci. Total Environ.*, 819, 153104, <https://doi.org/10.1016/j.scitotenv.2022.153104>, 2022.

745 Hsu, Y., Divita, F., Dorn, J.: SPECIATE 5.0 - Speciation Database Development Documentation, Final
746 Report, M. MENETREZ, Abt Associates Inc./Office of Research and Development/U.S.
747 Environmental Protection Agency Research Triangle Park, NC27711,
748 https://www.epa.gov/sites/default/files/2019-07/documents/speciate_5.0.pdf, 2019.

749 Huang, C. H., Hu, J. L., Xue, T., Xu, H., Wang, M.: High-Resolution Spatiotemporal Modeling for
750 Ambient PM_{2.5} Exposure Assessment in China from 2013 to 2019, *Environ. Sci. Technol.*, 55, 2152-
751 2162, <https://doi.org/10.1021/acs.est.0c05815>, 2021.

752 Huang, Z. J., Zheng, J. Y., Qu, J. M., Zhong, Z. M., Wu, Y. Q., Shao, M.: A Feasible Methodological
753 Framework for Uncertainty Analysis and Diagnosis of Atmospheric Chemical Transport Models,
754 *Environ. Sci. Technol.*, 53, 3110-3118, <https://doi.org/10.1021/acs.est.8b06326>, 2019.

755 Ji, Z., Gan, M., Fan, X., Chen, X., Li, Q., Lv, W., Tian, Y., Zhou, Y., Jiang, T.: Characteristics of PM_{2.5}
756 from iron ore sintering process: Influences of raw materials and controlling methods, *J. Clean. Prod.*,
757 148, 12-22, <https://doi.org/10.1016/j.jclepro.2017.01.103>, 2017.

758 Li, J., Wu, Y., Ren, L., Wang, W., Tao, J., Gao, Y., Li, G., Yang, X., Han, Z., Zhang, R.: Variation in PM_{2.5}
759 sources in central North China Plain during 2017–2019: Response to mitigation strategies, *J.*
760 *Environ. Manage.*, 28, 112370, <https://doi.org/10.1016/j.jenvman.2021.112370>, 2021.

761 Li, M., Hu, M., Du, B., Guo, Q., Tan, T., Zheng, J., Huang, X., He, L., Wu, Z., Guo, S.: Temporal and
762 spatial distribution of PM_{2.5} chemical composition in a coastal city of Southeast China, *Sci. Total*
763 *Environ.*, 605-606, 337-346, <https://doi.org/10.1016/j.scitotenv.2017.03.260>, 2017a.

764 Li, M., Liu, H., Geng, G., Hong, C., Liu, F., Song, Y., Tong, D., Zheng, B., Cui, H., Man, H., Zhang, Q.,

765 He, K.: Anthropogenic emission inventories in China: a review, *Natl. Sci. Rev.*, 4, 834-866,
766 <https://doi.org/10.1093/nsr/nwy044>, 2017b.

767 Li, X., He, K., Li, C., Yang, F., Zhao, Q., Ma, Y., Chen, Y., Ouyang, W., Chen, G.: PM_{2.5} mass, chemical
768 composition, and light extinction before and during the 2008 Beijing Olympics, *J. Geophys. Res.*,
769 118, 12158-12167, <https://doi.org/10.1002/2013JD020106>, 2013.

770 Liang, F., Xiao, Q., Yang, X., Liu, F., Li, J., Lu, X., Liu, Y., Gu, D.: The 17-y spatiotemporal trend of
771 PM_{2.5} and its mortality burden in China, *Proc. Natl. Acad. Sci.*, 117, 25601-25608,
772 <https://doi.org/10.1073/pnas.1919641117>, 2020.

773 Lv, L., Wei, P., Li, J., Hu, J.: Application of machine learning algorithms to improve numerical simulation
774 prediction of PM_{2.5} and chemical components, *Atmos. Pollut. Res.*, 12, 101211,
775 10.1016/j.apr.2021.101211, 2021.

776 NBS (National Bureau of Statistics of China): China Statistical Yearbook 2021,
777 <http://www.stats.gov.cn/tjsj/ndsj/2021/indexch.htm>, last access: 2022.

778 Peterson, G., Hogrefe, C., Corrigan, A., Neas, L., Mathur, R., Rappold, A.: Impact of Reductions in
779 Emissions from Major Source Sectors on Fine Particulate Matter-Related Cardiovascular Mortality,
780 *Environ. Health Persp.*, 128, 017005, <https://doi.org/10.1289/EHP5692>, 2020.

781 Qi, H., Cui, C., Zhao, T., Bai, Y., Liu, L.: Numerical simulation on the characteristics of PM_{2.5} heavy
782 pollution and the influence of weather system in Hubei Province in winter 2015 (In Chinese),
783 *Meteorological monthly*, 45, 1113-1122, <https://doi.org/10.7519/j.issn.1000-0526.2019.08.008>,
784 2019.

785 Seinfeld, J. H., Pandis, S. N.: Atmospheric Chemistry and Physics, from air pollution to climate change.
786 John Wiley & Sons, Inc., Hoboken, New Jersey.47-61, ISBN9781119221166, 2006

787 Sha, T., Ma, X., Jia, H., Tian, R., Chang, Y., Cao, F., Zhang, Y.: Aerosol chemical component: Simulations
788 with WRF-Chem and comparison with observations in Nanjing, *Atmos. Environ.*, 218, 1-14,
789 <https://doi.org/10.1016/j.atmosenv.2019.116982>, 2019.

790 Shi, W., Liu, C., Norback, D., Deng, Q., Huang, C., Qian, H., Zhang, X., Sundell, J., Zhang, Y., Li, B.,
791 Kan, H., Zhao, Z.: Effects of fine particulate matter and its constituents on childhood pneumonia: a
792 cross-sectional study in six Chinese cities, *Lancet*, 392, S79, [https://doi.org/10.1016/S0140-6736\(18\)32708-9](https://doi.org/10.1016/S0140-6736(18)32708-9), 2018.

794 Shi, Z., Li, J., Huang, L., Wang, P., Wu, L., Ying, Q., Zhang, H., Lu, L., Liu, X., Liao, H., Hu, J.: Source
795 apportionment of fine particulate matter in China in 2013 using a source-oriented chemical transport
796 model, *Sci. Total Environ.*, 601-602, 1476-1487, <https://doi.org/10.1016/j.scitotenv.2017.06.019>,
797 2017.

798 Song, S. Y., Wang, Y. S., Wang, Y. L., Wang, T., Tan, H. Z.: The characteristics of particulate matter and
799 optical properties of Brown carbon in air lean condition related to residential coal combustion,
800 *Powder Technol.*, 379, 505-514, <https://doi.org/10.1016/j.powtec.2020.10.082>, 2021.

801 Tang, X. Y., Zhang, Y. H., Shao, M.: Atmosphere Environment Chemistry, Second ed (In Chinese). .
802 Higher Education Press, Beijing, China.268-329, ISBN978-7-04-019361-9, 2006

803 Wang, C., Zheng, J., Du, J., Wang, G., Klemes, J., Wang, B., Liao, Q., Liang, Y.: Weather condition-
804 based hybrid models for multiple air pollutants forecasting and minimisation, *J. Clean. Prod.*, 352,
805 131610, <https://doi.org/10.1016/j.jclepro.2022.131610>, 2022.

806 Wang, D., Hu, J., Xu, Y., Lv, D., Xie, X., Kleeman, M., Xing, J., Zhang, H., Ying, Q.: Source
807 contributions to primary and secondary inorganic particulate matter during a severe wintertime
808 PM_{2.5} pollution episode in Xi'an, China, *Atmos. Environ.*, 97, 182-194,

809 <https://doi.org/10.1016/j.atmosenv.2014.08.020>, 2014.

810 Weagle, C., Sinder, G., Li, C. C., Donkelaar, A., S, P., Bissonnette, P., Burke, I., Jackson, J., Latimer, R.,
811 Stone, E., Abboud, I., Akoshile, C., Anh, N., Brook, J., Cohen, A., Dong, J., Gibson, M., Griffith,
812 D., He, K., Holben, B., Kahn, R., Keller, C., Kim, J., Lagrosas, N., Lestari, P., Khian, Y., Liu, Y.,
813 Marais, E., Martins, J., Misra, A., Muliane, U., Pratiwi, R., Quel, E., Salam, A., Segey, L., Tripathi,
814 S., Wang, C., Zhang, Q., Brauer, M., Rudich, Y., Martin, R.: Global Sources of Fine Particulate
815 Matter: Interpretation of PM_{2.5} Chemical Composition Observed by SPARTAN using a Global
816 Chemical Transport Model, *Environ. Sci. Technol.*, 52, 11670-11681,
817 <https://doi.org/10.1021/acs.est.8b01658>, 2018.

818 Wongphatarakul, V., Friedlander, S. K., Pinto, J. P.: A Comparative Study of PM_{2.5} Ambient Aerosol
819 Chemical Databases, *Environ. Sci. Technol.*, 32, 3926-3934, <https://doi.org/10.1021/es9800582>,
820 1998.

821 Wu, B., Bai, X., Liu, W., Zhu, C., Hao, Y., Lin, S., Liu, S., Luo, L., Liu, X., Zhao, S., Hao, J., Tian, H.:
822 Variation characteristics of final size-segregated PM emissions from ultralow emission coal-fired
823 power plants in China, *Environ. Pollut.*, 259, 113886, <https://doi.org/10.1016/j.envpol.2019.113886>,
824 2020.

825 Wu, D., Zheng, H., Li, Q., Jin, L., Lyu, R., Ding, X., Huo, Y., Zhao, B., Jiang, J., Chen, J., Li, X., Wang,
826 S.: Toxic potency-adjusted control of air pollution for solid fuel combustion, *Nat. Energy*, 7, 194-
827 202, <https://doi.org/10.1038/s41560-021-00951-1>, 2022.

828 Wu, Z. X., Hu, T. F., Hu, W., Shao, L. Y., Sun, Y. Z., Xue, F. L., Niu, H. Y.: Evolution in physicochemical
829 properties of fine particles emitted from residential coal combustion based on chamber experiment,
830 *Gondwana Res.*, <https://doi.org/10.1016/j.gr.2021.10.017>, 2021.

831 Xia, Z. Q., Fan, X. L., Huang, Z. J., Liu, Y. C., Yin, X. H., Ye, X., Zheng, J. Y.: Comparison of Domestic
832 and Foreign PM_{2.5} Source Profiles and Influence on Air Quality Simulation (In Chinese), *Res.*
833 *Environ. Sci.*, 30, 359-367, <https://doi.org/10.13198/j.issn.1001-6929.2017.01.55>, 2017.

834 Yang, F., Tan, J., Zhao, Q., Du, Z., He, K., Ma, Y., Duan, F., Chen, G., Zhao, Q.: Characteristics of PM_{2.5}
835 speciation in representative megacities and across China, *Atmos. Chem. Phys.*, 11, 1025-1051,
836 <https://doi.org/10.5194/acpd-11-1025-2011>, 2011.

837 Ying, Q., Feng, M., Song, D. L., Wu, L., Hu, J., Zhang, H., Kleeman, M., Li, X.: Improve regional
838 distribution and source apportionment of PM_{2.5} trace elements in China using inventory-observation
839 constrained emission factors, *Sci. Total Environ.*, 624, 355-365,
840 <https://doi.org/10.1016/j.scitotenv.2017.12.138>, 2018.

841 Yu, Z. C., Jang, M., Kim, S., Bae, C., Koo, B., Beardsley, R., Park, J., Chang, L., Lee, H., Lim, Y., Cho,
842 J.: Simulating the Impact of Long-Range-Transported Asian Mineral Dust on the Formation of
843 Sulfate and Nitrate during the KORUS-AQ Campaign, *Earth Space Chem.*, 4, 1039-1049,
844 <https://doi.org/10.1021/acsearthspacechem.0c00074>, 2020.

845 Zhang, J., Wu, J., Lv, R., Song, D., Huang, F., Zhang, Y., Feng, Y.: Influence of Typical Desulfurization
846 Process on Flue Gas Particulate Matter of Coal-fired Boilers (In Chinese), *Environ. Sci.*, 41, 4455-
847 4461, <https://doi.org/10.13227/j.hjcx.202003193>, 2020.

848 Zhang, Q., Xue, D., Wang, S., Wang, L., Wang, J., Ma, Y., Liu, X.: Analysis on the evolution of PM_{2.5}
849 heavy air pollution process in Qingdao (In Chinese), *China Environ. Sci.*, 37, 3623-3635,
850 <https://doi.org/10.3969/j.issn.1000-6923.2017.10.003>, 2017.

851 Zhang, S. P., Xing, J., Sarwar, G., Ge, Y. L., He, H., Duan, F., Zhao, Y., He, K., Zhu, L., Chu, B.:
852 Parameterization of heterogeneous reaction of SO₂ to sulfate on dust with coexistence of NH₃ and

853 NO₂ under different humidity conditions, *Atmos. Environ.*, 208, 133-140,
854 <https://doi.org/10.1016/j.atmosenv.2019.04.004>, 2019.

855 Zheng, B., Tong, D., Li, M., Liu, F., Hong, C., Geng, G., Li, H., Li, X., Peng, L., Qi, J., Yan, L., Zhang,
856 Y., Zhao, H., Zheng, Y., He, K., Zhang, Q.: Trends in China's anthropogenic emissions since 2010
857 as the consequence of clean air actions, *Atmos. Chem. Phys.*, 18, 14095-14111,
858 <https://doi.org/10.5194/acp-18-14095-2018>, 2018.

859 Zheng, B., Zhang, Q., Zhang, Y., He, K. B., Wang, K., Zheng, G. J., Duan, F. K., Ma, Y. L., Kimoto, T.:
860 Heterogeneous chemistry: a mechanism missing in current models to explain secondary inorganic
861 aerosol formation during the January 2013 haze episode in North China, *Atmos. Chem. Phys.*, 15,
862 2031–2049, 10.5194/acp-15-2031-2015, 2015.

863 Zheng, H., Song, S., Sarwar, G., Gen, M., Wang, S., Ding, D., Chang, X., Zhang, S., Xing, J., Sun, Y. L.,
864 Ji, D., Chan, C. K., Gao, J., McElroy, M.: Contribution of Particulate Nitrate Photolysis to
865 Heterogeneous Sulfate Formation for Winter Haze in China, *Environ. Sci. Technol. Lett.*, 7, 632-
866 638, <https://doi.org/10.1021/acs.estlett.0c00368>, 2020.

867 Zhou, L., Chen, X., Tian, X.: The impact of fine particulate matter (PM_{2.5}) on China's agricultural
868 production from 2001 to 2010, *J. Clean. Prod.*, 178, 133-141,
869 <https://doi.org/10.1016/j.jclepro.2017.12.204>, 2018.

870